Endoparasite Home-Test

Detecting different particles by size-based separation and optical detection

Project Group B Lab-on-a-Chip
Floor Couwenberg (s1577921)
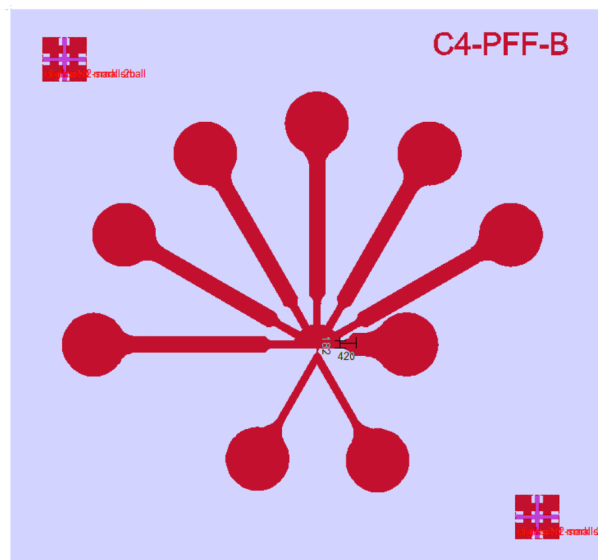Marieke Meteling (s1584472)
Irnti Nousi (s1465376)
Jasper Ringoot (s1579746)
Kwan Suppaiboonsuk (s1537229)

Supervisors
Prof. dr. Jan Eijkel
PhD. Joshua Loessberg-Zahl

Abstract

This paper provides a background for the design of a microfluidic chip for creating a endoparasite home-testing device for horses. In the paper an experimental set-up and method is introduced for testing the performance of pinched flow fractionation (PFF) for separation and photoresistors for optical detection. The PFF is used for separating beads (comparable to parasite eggs) and is tested at different flow rate ratios and multiple images are taken for analysis. The photoresistors are tested to see the viability in measuring the concentration of beads in a solution (severity of parasitic infection). The results from these tests are discussed within this paper. Further recommendations for future research and applications are also provided.

Contents

1   Introduction

Horses and other domestic animals have to cope with loads of parasites and diseases. Most of these infections are dealt with by their immune system and for those infections that do slip through, humans invented antibiotics. But simply giving antibiotics is not always the solution. Animals can suffer quite a bit from the antibiotics and parasites can eventually become immune against anthelmintic drugs as well.

In this report one group of infections is analysed specifically for horses. Worm infestations are known to be a reason for health, growth and weight loss problems. Diarrhoea, severe intestinal cramps and even the death of a horse are not unusual results when infested by these parasites. Common types of this worm group with their respective egg sizes are given in Table 1. These parasites live within the gastrointestinal tract and cause the aforementioned problems [1]. Tapeworms are found in the intestine of horses as well, but are considered not so harmful and next to that are not found in horse faeces [2].

Parasital egg sort	Egg size
Roundworms (Ascarids)	90 - 100 μm diameter
Bloodworms (Strongyles Vulgares)	60-120 μm X 35-60 μm
Threadworm (Nematodes)	40-52 μm X 32-40 μm
Pinworms (Oxyuris Equi)	85-95 μm X 40-45 μm

Table 1: Typical intestinal horse parasites and their respective sizes [3]

Anthelmintics is the drug given to treat such infestations. Many horses are given a dose as prevention, but without knowing for sure that the horse is indeed infested by worms. Diagnosis is expensive compared to the selling price of anthelmintics. This is why many horse owners simply use the anthelmintics and hope that their animal can cope with the side-effects.

The current procedure to determine if a horse is infected by worms is that the owner takes a sample of the horse's faeces and sends this to the veterinarian. The veterinarian will then use a floating technique where the sample is mixed with a suspension median of which the density is higher than that of the parasites. Most parasite eggs have a specific gravity (SG) between 1.05 and 1.23. Common suspension medians are: saturated sodium chloride (NaCl; SG 1.18), sugar (Sheather's solution; SG 1.27 to 1.33), sodium nitrate (NaNO3; SG 1.18 to 1.20), magnesium sulfate (MgSO4; SG 1.20), and zinc sulfate (ZnSO4; SG 1.20) [4]. These fluids will make the parasites float and makes them separable from the rest of the sample. This separation can be sped up by using a spinning system which will push the denser particles to the bottom and the lighter eggs to the top. Next, the parasites are counted and identified under a microscope to determine the severity of the infection.

For the floating method it was found that counts of 1.2 eggs/μL are considered high egg counts, while 0.2 eggs/μL are low egg counts. With the former value, the horses will need proper treatment; the latter value is usually what should be the outcome measurement after a treatment. No treatment is necessary at egg count of 0.05 eggs/μL or lower. The detection limit usually lies at 0.025 eggs/μL [5].

Both horse and owner would benefit from a method where the horse could be investigated prior to the treatment. A system that could provide a solution could be a lab-on-a-chip. These systems perform laboratory operations on a very small scale. These chips distinguish themselves by requiring little resources, produce almost no waste, and can be bulk-produced, which greatly reduces the total costs as well [6].

The aim for this report is to investigate and test the possibilities of creating a lab-on-a-chip with which the diagnosis is done at the horse owner's home. This device must replace the current expensive analysis and at the same time be cheaper than the anthelmintics. So that every horse is tested before being injected with an anthelmintic drugs.

2 Theory

2.1 Separation techniques

Literature research was done to find a suitable separation method for the separation of the parasite eggs on a 'lab-on-a-chip' device. As the device is supposed to function as a home-test, the faecal sample should need as little preparation as possible. Therefore, the focus was on label-free sorting methods, which were again narrowed down to passive sorting techniques, as the parasite eggs do not have any magnetic or intrinsic dielectric properties, to our knowledge [7].

Further investigation of the passive sorting methods led to the choice of pinched flow fractionation (PFF). Both inertial focusing and PFF seem to be the most suitable choices, but as the spiral channel used for inertial focusing takes up more than five times of space compared to the PFF channels, this would result in a chip of more than nine squared centimetres, thus, PFF is more suitable. For further detail on this choice the project plan can be consulted.

2.1.1 Pinched flow fractionation

The pinched flow fractionation sorts particles based on size. First the particles that are to be sorted are led through one inlet that is intersected by another inlet. Both merge to one channel that is, so to say 'pinched', so the cross-section is smaller compared to the cross-sections of the two inlet channels [7, 8]. The second inlet channel (Figure 1) supplies the system with a buffer solution that has a higher flow rate than the particles [9]. Because of the higher flow rate of the buffer solution, the particles are pushed against one side wall. Together with the smaller cross-section of the pinched segment that acts as a constraint to the particles, it causes the particles to align onto the side wall. Aligned, the particles reach depending on their size, into different areas of the flow profile. The pinched segment is rather short and quickly broadens into a comparatively wide channel. In the broadening segment, the cells separate based on size because of the laminar flow profile. This effect can already be seen without the intersecting buffer solution, but through this buffer solution with a higher flow rate the separation is enhanced [7].
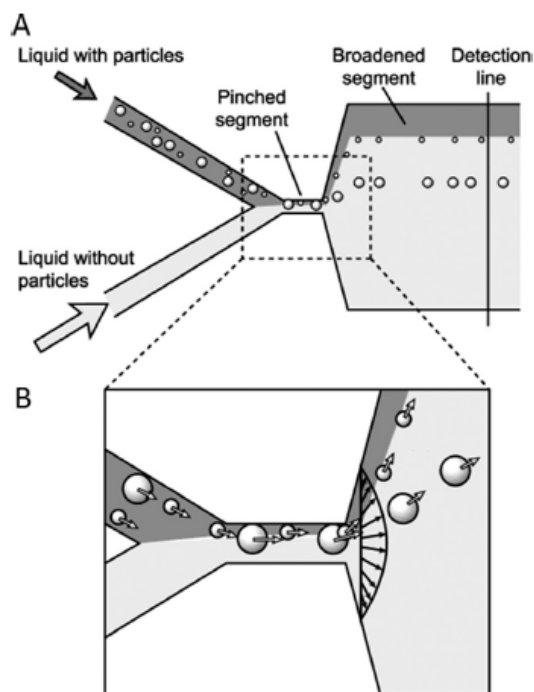

Figure 1: Pinched flow fractionation (PFF). (A) Schematic drawing of PPF, (B) Magnification of the pinched segment and the first part of the broadening channel. From Yamada et al. *Anal. Chem.* 2004 [8]

2.1.2 Back-up technique

As mentioned above the inertial focusing is a promising candidate for the separation as well. Therefore, it is our back-up should the PFF not work well. Inertial focusing makes use of a spiral microchannel (Figure 2) and the separation of particles is based on inertial migration [10].

In straight channels, particles already migrate to a sort of equilibrium position due to several forces, no matter what their position is at the inlet. This is caused by the parabolic velocity profile of laminar flow through a straight channel. The particles are pushed away from the center of the channel and closer to the channel wall due to an inertial lift force resultant from the shear gradient. However when they get near the wall, the particles experience another force that pushes them back to the center of the channel. These two forces together create a *net lift force*, which is a function of (among others) the size of the particle [12, 11]. In a curved rectangular channel the parabolic velocity profile of a straight channel is shifted such that the maximum velocity is closer to the concave channel wall [12]. The centrifugal force
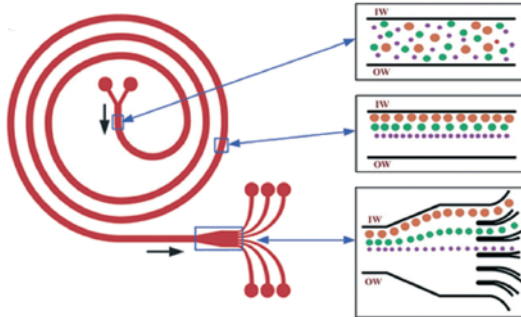

Figure 2: Schematic drawing of the spiral flow principle. From Kuntaegowdanahalli et al. *Lab chip* 2009 [11]

that follows from the curvature results in two vortices called the *Dean vortices*. Because of these vortices the particles experience a *Dean drag*, which is opposite to the net lift force. The equilibrium position of the particles depends on the ratio of the net lift force to the Dean drag. Since this ratio is dependent on the size of the particle to the third power, size-based separation is possible [11].

2.2 Filtration techniques

Aside from the parasite eggs, the faecal sample contains a lot of unwanted debris. Simply putting the faeces into a solution and filtering everything before a sample is put into the chip is not an option as the eggs would be filtered out as well or a lot of debris would still get through. Apart from that it would mean extra work for the user.

Several in-chip filtration methods exist. The important point in our case is that the larger particles, the parasitic eggs, need to get through, while the smaller particles, like dust particles, need to be filtered out. This already rules out any kind of filtration using large barriers, like weirs, membranes or pillars, designed to trap the larger particles [7]. Hydrodynamic filtration was found to be most suitable. For more information on this the project plan can be consulted.

2.3 Integrated filtration

An alternative to an actual extra filtration step in the chip would be to implement it into the separation part. This is possible with the chosen separation technique, the PFF. Instead of splitting the broadening segment into as twice as many collecting channels as eggs that need to be sorted, but into at least two more. This one would be for all the particles smaller than the parasitic eggs. There could be another one for particles larger than the parasitic eggs as well, in the case that the faecal sample is only poorly filtered before hand. This method might be less precise, but is a lot easier to produce. Therefore, it was chosen to integrate the filtration in the separation part and only use the hydrodynamic filtration as back-up.

2.4 Detection techniques

Literature research was also done to find a suitable method to detect the amount of parasite eggs in the sample, which determines the severity of the parasite infection. In veterinarian clinics, the method that is being used is manual counting of the eggs under a microscope. As this is not an efficient method for the user, two other methods are considered: optical detection and electrical detection. These methods are further discussed in the sections below, with optical detection being determined as the most optimal for this design. That is because, in order to fabricate the desired size of electrodes, the clean room needs to be used, which is not allowed for this project. Some other detection methods also considered are pH concentration and color identification but were disregarded as it is either not possible or requires further research beyond the scope of this project.

2.4.1 Optical detection

Optical detection is getting more and more popular on the field of LOC. There are a few categories of optical detection like absorbance, fluorescence or chemiluminescence detection. All of them rely on measuring a direct change in the light intensity. For our project absorbance detection will be discussed further. This method can be realized by the use of a LED coupled with a phototranistor. The LED is the light source which will generate light towards the microfluidic channel and the phototransistor is the detector which converts the light into current. Such a set up can be seen in the figure below.
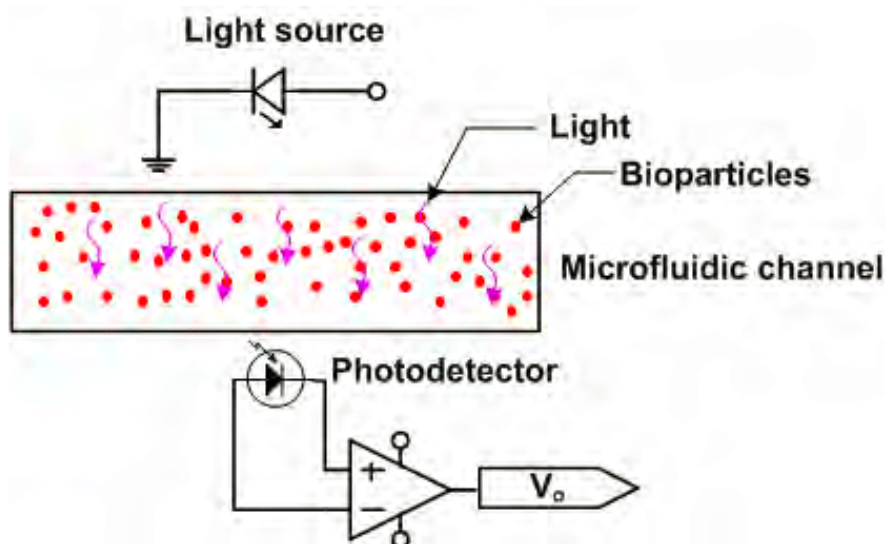

Figure 7: Oprical detection using absorbance method

The first step in the process will be to guide the light through the solution, which contains no eggs, and with the phototransistor translate that light intensity into a current. Next step will be to perform the same measurement by using a solution which contains a concentration of eggs which is just above the normal. The light intensity will change, which means a different value of current. Those two different values of current can be used as the boundaries. Any value above that will indicate that the horse is diseased and any value between the boundaries will indicate that the horse is healthy.

There are five different channels that need to be measured. For each channel a different phototransistor is going to be used. The phototransistors will be placed on the top of the channels. On the bottom there will be five light sources. For each light source there will be a guidance to focus the light into the channel.

2.4.2 Electrical detection

Another method of detection is by using electrodes to generate a current and field, which can be used to perform analysis of the solution. Each time a particle passes between the electrodes, there is a disruption in the field. This disruption can be used to count the amount of parasitical eggs in the solution, as a program can be written to count for each time the field fluctuates. As detection via electric fields are more specific towards an object passing through an area, it allows for more accurate counting as opposed to optical detection, which analyses the amount concentration based on an area. Even though the method of electrical detection can produce high accuracy results, the drawbacks are in the collection of substance at the electrodes (see Appendix: Table of Detection Methods) [13]. The production of heat due to electrodes is also a point of concern, as heat can incubate the eggs in the channel and cause hatching. Hatching of parasites is not desirable as it could clog and ruin the chip. The use of electrodes within this project is also not feasible, as access to a clean room is needed for fabrication. As this method is deemed infeasible for this project, the theory behind the method is not looked into extensively in detail.

3   Modelling & Design

Prior to having testable LOCs, one must first come up with a design. This design can be made in multiple programs, each with their own application. Clewin is the program which is primarily used by the MESA+ groups to design masks. With micron accuracy these designs can prove themselves very useful, but they have their respective price as well. Where 500 Euro is not uncommon for a basic photomask.

Another option would be to use Solidworks for either micro milling or 3D printing. As micro milling is not accurate enough for the purpose of this project, Solidworks was applied in the creation of 3D printing designs. With bottom accuracy at a 100 microns it is less precise but on the other hand a whole lot cheaper and quicker as a photomask. In this particular case Solidworks in combination with a 3D printer was used to create a design that would suit larger 75 μm beads.

Both programs and the chip designs created with them are explained in detail in the sections below. The exact reasoning on why the upcoming designs were chosen can be found in the previous report: Endoparasite Home-test Project Plan.

3.1   Clewin designs for lithography

Clewin has multiple distinctive features that include: hierarchy, true-type fonts and boolean operations. All these features make designing and repeating difficult shapes easy applicable.

In total six different chip designs were made in Clewin. In Figure 3 an overview of all the chips is given. Where the bottom four designs are primarily to test PFF. With the middle ones testing a symmetric outlet channel length and the outer ones an asymmetric division. One may notice that the top two designs on the right are equal in shape but the left of the two has the design duplicated. These designs are added so that testing with the photo transistors can be performed in mono and duplo. As these seven designs will not occupy half of the photomask completely, the remaining space is filled with multiple copies of the aforementioned designs. This makes it easier to create multiple chips with one PDMS mould.
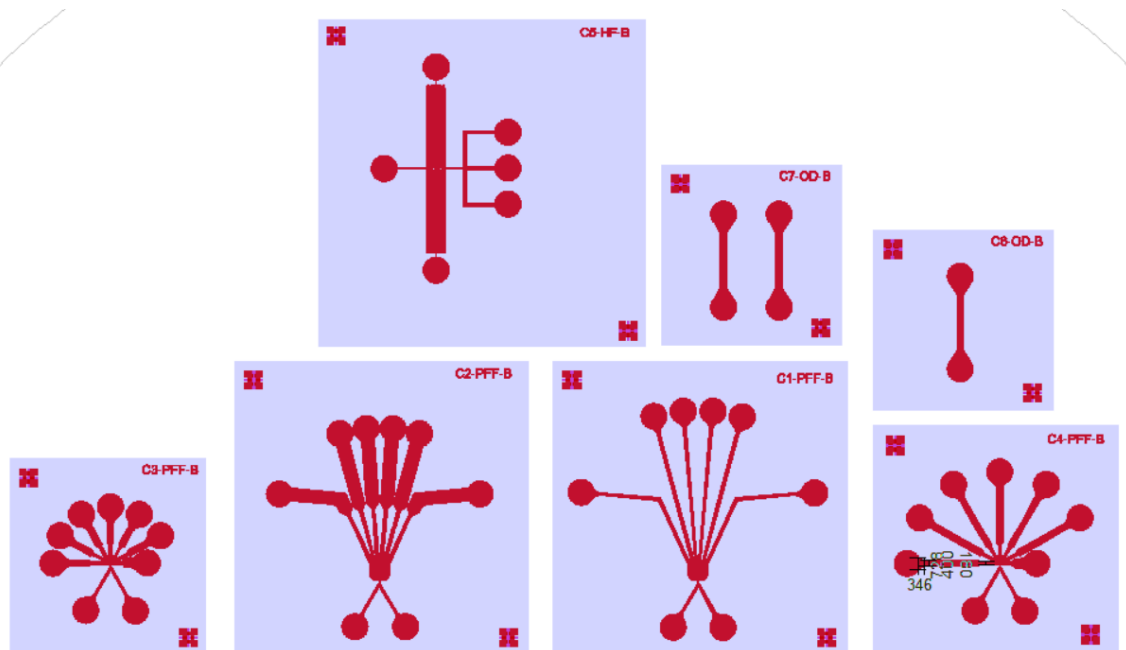

Figure 3: Overview of all chips designed in Clewin

Figure 4 displays a close up of one of the chips. Here one can see square like markers given in the top left and bottom right corner. These markers are added in to assist the alignment of the machines in the Nanolab.
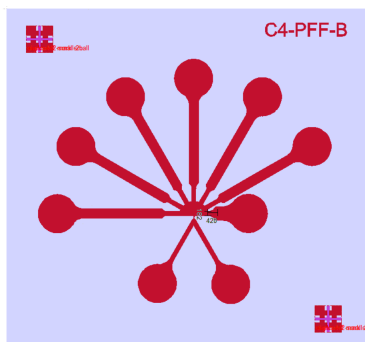

Figure 4: Close up of one Clewin designed chip

3.2 Solidworks designs for 3D printing

Different to Clewin, Solidworks is more well-known and has many more applications and options. It's main purpose is to create 3D designs and objects. Most of the time one starts off with creating a sketch in 2D. Each line, circle or other shape has certain dimensions and relations which makes it possible to create very detailed and precise designs. One example of these 2D designs can be found in Figure 5.

After a 2D design is fully defined one can easily make it into a 3D object by extruding the sketch. A 3D object has even more shape altering options where the true potential of Solidworks comes into play. In Figure 6 all three of the 3D printing designs are displayed. Where the left two are remade designs from Clewin and the right chip displays a spiral flow. Each chip has a lofted base underneath which makes removal from the 3D printing plate easier and prevents cracks during removal. Each chip has raised walls acting as a container for the PDMS to be poured in. The chip designs within the so called container are raised 150 microns to create the channels when the PDMS hardens.
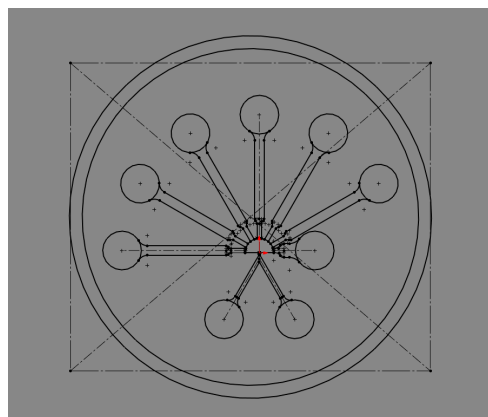

Figure 5: 2D sketch in Solidworks

All three designs are saved in the correct file type and send to the 3D printer for fabrication.
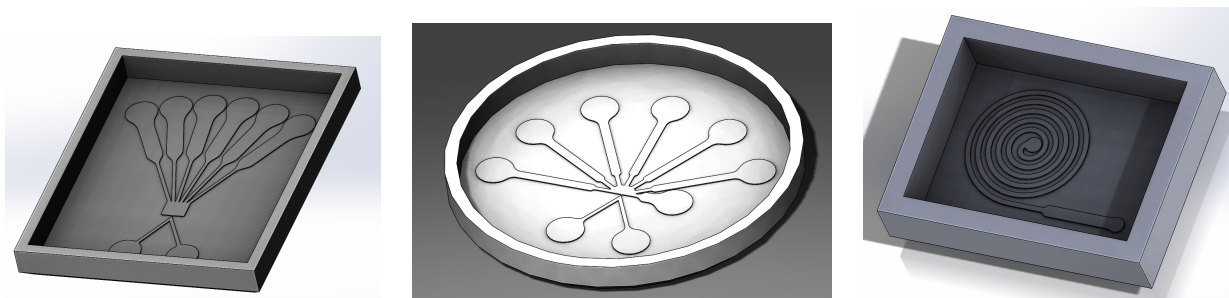

Figure 6: Three 3D designs made in Solidworks for 3D printing

3.3 Design of the set-up and electric circuit

The set up designed for testing the optical detection was to connect the resistor in series with the LED on one breadboard and fix it on the top side of the channel, so that it is shining light through to the other side, where the the sensor was. The sensor was placed on a different breadboard, in series with the a resistor and the multimeter. Between the breadboards some plastic plates where placed in order to keep the distance between the light source and the sensor constant. The distance was kept as short as possible in order decrease the effect of other factors such as reflection. Everything was taped together and placed in a non-transparent box with a lid, preventing the photoresistor from outside noise due to other light sources within the environment. The schematic of the set up, in side view, can be seen in Figure 7.
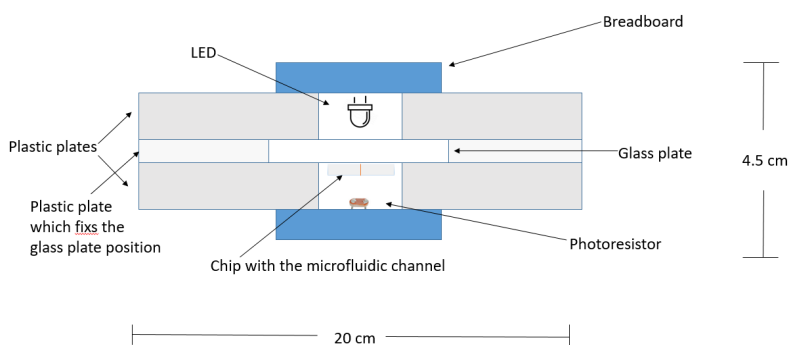
Figure 7: Schematic of the electrical detection set up.

To further prevent noise due to the scattered light from the system, aluminum foil was placed around the LED. Now the light from the LED is also more focused, therefore a higher intensity of light is propagating through the channel. Moreover, a cone made of aluminum foil was placed on the top of the phototransistor. By doing so, the sensor is focused sensing the light intensity passing only through the channel of the chip and therefore making the detection of the particles more accurate. The light that the phototransistor senses is also mostly from the system itself, providing a more accurate reading in transmittance. The final set up can be seen in figure 8.
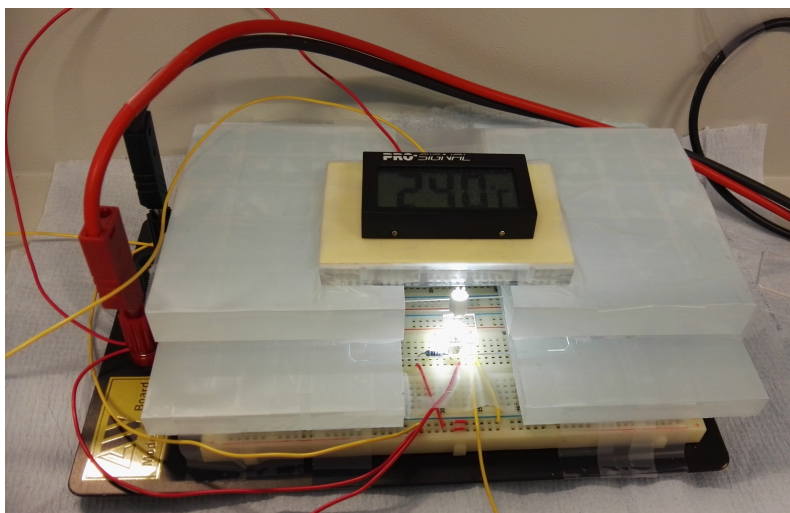
Figure 8: Picture of electrical detection set up.

Searching on how to improve the detection and increase the absorbance, the Beer-Lambert Law was found. The mathematical equation is $A = \epsilon \cdot L \cdot C$,where ϵ is the molar absorbtivity, L is the height of the channel for this case and C is the concentration of the compound in solution. From the equation it can be seen that increasing L will also give higher value of absorbance. In order to test if that was true in this system, a new design would be necessary. A new design was not possible to be made since it requires a large process(including new photomask and lithography). So, instead a plastic tube was used as a channel.

The electric circuit that was designed in order to realize the optical detection can be seen in figure 9. It consists of two resistors, a LED that works as the light source, a photoresistor which is the sensor, a power supply to get the desired DC volt, and a multimeter which was used to measure the current.

Figure 9: The schematic of the electric circuit.

4 Experimental

4.1 Microdevice fabrication

For both 6 and 20 μm beads a negative photoresist, SU-8, was spin-coated on a silicon wafer to achieve a layer with a thickness of 50 μm. A photomask was made inside the Nanolab of the University of Twente according to the designs made in Clewin that were mentioned i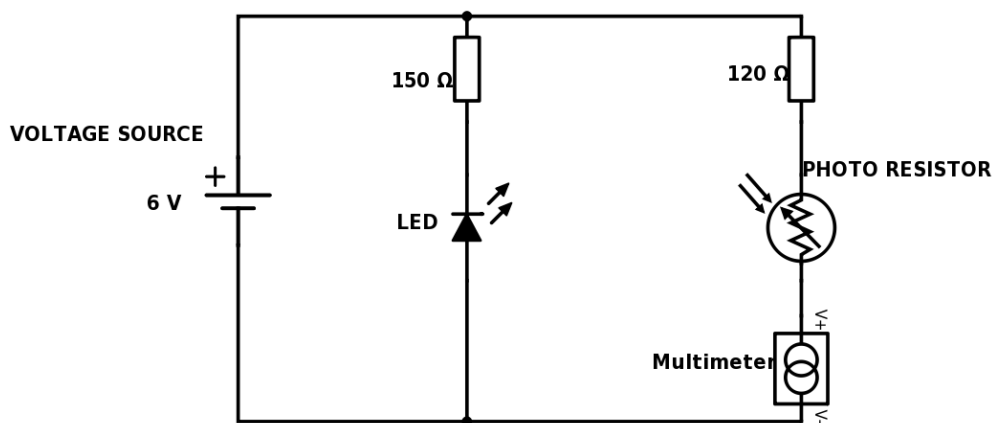n section 3.1. The photomask was put on top of the SU-8 after which it was exposed to UV-light to make the desired channels. After removal of the excess SU-8 and development of the wafer, the PDMS is cast over the SU-8 mold and cured. After this the PDMS is peeled off the mould, inlets and outlets are punctured in the designated spots, and after a treatment in the plasma oven, the chip is bonded to a rectangular microscope glass. For the detailed step by step instruction one can look in the Module 10 Lab and fabrication skills & project manual.

To perform tests with the 75 μm beads, a mould is 3D printed instead of using the SU-8 and the photomask. This is because when using beads of this size, the channels have to be higher than 50 μm, which is about the maximum you can get with the SU-8 coating. The moulds were constructed in *Solidworks* based on the designs made in Clewin. After the chips are 3D printed the PDMS could be poured over and the remainder of the process is identical to the previous method with SU-8. Further information about the exact shapes and designs made in Solidworks can be found in section 3.2.

After the moulds were created in the 3D printer. It turned out that the left two designs in Figure 6 had either outlets or one outlet and a channel merged together. Which made them unusable as a PDMS mould. The third spiral flow design cracked during removal from the 3D printing plate, deeming it unusable as well. Due to time limitation and the lack of 3D printing fluid, any further attempt at making new designs was a waste of time. This resulted in the lithography chips being the only ones used for testing.

4.2 Preparation of bead solution

There are different sizes of beads, each with their own concentration. As mentioned before the different sizes include 6, 20 and 75 microns in diameter. Due to failure in the 3D printing process the 75 micron beads were not needed any more and only the 6 and 20 micron beads needed preparation. The microbeads are produced by a company called Polysciences, Inc. and both have a concentration of 2.66% of microbeads. The remainder is filled with demiwater.

As the beads have a higher density than that of demiwater, they would sink and have to be properly shaken and tapped in order to spread them throughout any liquid. Presented in their current form the concentration of the bead solution would still be far to high. Thus further dilution with demiwater is necessary. Next to this further dilution with another solution, Tween 20, is added which will reduce the sticking of beads in the syringes, tubing and microchip itself. All these volumes of water can be related to a certain bead concentration. The following calculations will elaborate on the exact determination of volume division.

The determination for the volume of just the beads can be done through their radii of both 3 and 9 microns. Assuming the beads are perfect spheres their volume can be calculated through $4/3 * \pi * r^3$ which results in $113.1 \mu m^3/bead$ and $3053.6 \ \mu m^3/bead$ respectively. As $1 \ \mu L = 1 \ mm^3$, the respective units after conversion are $1.131 * 10^{-7} \ \mu L/bead$ and $3.0536 * 10^{-6} \ \mu L/bead$.
As concentration is usually given by $bead/\mu L$ the obtained number needs conversion again. Now taking in mind as well that the concentration of beads was only 2.66 % the end concentration needs to be multiplied by 0.0266 as well. Giving:

$$\frac{1 * 0.0266}{1.131 * 10^{-7} \mu L/bead} \approx 235190 \ beads/\mu L \quad \& \quad \frac{1 * 0.0266}{3.0536 * 10^{-6} \mu L/bead} \approx 8515 \ beads/\mu L$$

Where the first 6 micron bead concentration consisted of 4600 $beads/\mu L$ the mixed 6 and 20 micron solution has a preferred concentration of 9200 $beads/\mu L$. This was rounded to 9000 $beads/\mu L$.

Assuming one uses a full syringe of 500 μL the desired volume can be calculated through:

$$\frac{235190 \ beads/\mu L * X \ \mu L}{500 \ \mu L} = 9000 \ beads/\mu L \quad \& \quad \frac{6350 \ beads/\mu L * Y \ \mu L}{500 \ \mu L} = 9000 \ beads/\mu L$$

Which results in $X \approx 19.13 \ \mu L$ and $Y \approx 528 \ \mu L$.

When one only has a syringe of 500 μL the volume of Y is too much. Scaling down to a total volume of 150 μL would still result in approximately 158 μL, which is still quite a lot for the available resources of the 20 microbead solution. It turned out that there was only 40 μL to be obtained from the stock solution. Which when calculated the other way around resulted in a concentration of 2270 beads/μL.

To achieve a concentration of 2270 beads/μL for the 6 micron beads for a total volume of 150 μL, one needs 1.45 μL of stock solution.

Tween 20's stock solution has a 1:5 ratio between the Tween and the demiwater. Through consultancy of our daily tutor the maximum concentration of Tween that could be present in the bead solution was 2 % of the total volume. $150 * 0.02 = 3$ is the result but as it is diluted by itself the maximum is set at 15 μL. The first bead solution contained 3.75 μL and was determined to be too little as the beads got stuck too much inside the syringe and chips. Hence the scaling up of the concentration Tween present.

With 10 μL of Tween added this leaves a total of $150 - 10 - 1.45 - 40 = 98.55 \ \mu L$ of demiwater to be added.

4.3 Measurement methods

In the following section, the experimental set-up and methods are explained for testing the separation of beads and testing of the optical detection for counting beads.

4.3.1 Separation

Hypothesis

There is an optimal flow rate at which the beads are all pushed and aligned against the pinched segment wall. Once in the broadening segment, the beads should flow more or less in one line.

Set-Up

To set up the testing for the separation with pinched flow fractionation (PFF), in order for the chip to be tested it is placed on the microscope, with the camera turned on for desktop computer view. Two syringes are well-prepared and placed on the syringe pump, one filled with water and the other filled with the bead solution. The syringe pump is properly calibrated and tubes are attached to the syringe for connection to the chip inlet holes. Equal lengths of tubing are also inserted into all the outlet holes to prevent the overflow of liquid out of the channels. This also allows for control over the resistance within the outlet channels.

Methods

With the set-up mentioned, the following steps were followed to test the different flow ratios (see table 2). These different rates are tested to find the best environment for optimal separation of different size of beads (comparable to different size of parasite eggs) - and to test if the chosen separation method works at all.

Table 2: Flow rates and ratios to be tested

Ratio	Flow rate bead solution (uL/hr)	Flow rate buffer (uL/hr)
1:8	200	1600
1:8	50	400
1:5	200	1000
1:6	20	120
1:10	200	2000
1:20	50	1000
1:6	500	3000

1. Insert the tube from the water syringe into one of the inlet holes. Run the water through the chip. If the water flow is diverted prior to the pinched flow segment, the tube from the syringe with the bead solution will have to be inserted into the other inlet hole. In order to prevent as much bubbles within the chip as possible, prior to inserting the tube from the bead solution syringe, run the pump until a small droplet of bead solution shows up at the end of the tube. The water syringe pump should be stopped, then the tube for the bead solution can be inserted into the inlet hole. Continue pumping the water until the whole chip is filled.

2. Look through the microscope camera to see if there are any bubbles or dusts in the chip which may be affecting the flow resistance. Remove as much bubbles as possible. This can be done by using tweezers to poke at the chip from the outside or if there are bubbles in the extended tubes in the outlets, capillary pressure can be used by closing off tubes without bubbles while leaving the syringe pump on. If bubbles are not removable, make sure that it does not completely block a channel, otherwise the chip is not usable.

3. Once satisfied with chip conditions, run the syringe pump for water and beads at the desired rate (see table below for flow rate ratio testing). Notice the streamline of the beads in the broadening segment to see how well they are being separated. Investigate the influence of different flow rates and ratios.

4. Make movies of the different ratios tested and save them in tiff format (frame rate 125).

5. If a chip has large or multiple slightly blocking the outlet channels, the resistance in that channel is then higher and not equal to the other outlet channels. To accommodate for this the extended tube from this outlet can be made shorter by cutting to lower the resistance.

4.3.2 Optical Detection

Hypothesis

It is expected that there will be limits to the sensor sensitivity, but changes in the amount of beads passing through will still be detected well enough, as the change current fluctuation will be noticeable. The higher the concentration the lower the current (mADC).

Methods

To measure the performance of the phototransistors' function in counting the amount of beads, the following measurement steps were followed with the described set up.

1. Turn on the power supply and let the set up warm up for a little while (ten to fifteen minutes), in order to reduce the drift in the measurements.

2. Turn off power supply as safety protocol and insert a plain glass slide into the designated chip slot of the set up.

3. Turn the power supply on, note down the temperature in the set-up, close the lid of the box and wait for one minute. Look at the measurement value of the current (mADC) and write it down. Open the lid of the box and note down the final temperature in the set-up for the measurement.

4. Turn off the power supply for safety protocol. Remove the slide, then insert a glass slide with an empty chip. Align the slide so that the light is focused on the empty channel and goes through to the phototransistor. Do the same as the previous step to get the measurement values and record it.

5. Perform the measurements with the same steps above. This should all be measured with the same chip. To add the liquids, use a micropipette to fill the channels with liquid (pipette 10 microlitres of liquid and stick the end of the tips through an inlet/outlet hole and fill the whole channel until liquid shows up on the other outlet/inlet hole.) Make sure there are no droplets on any inlet or outlet hole by carefully wiping them off with a paper towel.

4.4 Data analysis

4.4.1 Image processing

Intensity plots

To investigate the effect of the flow rates on the separation, recordings were made at 125 frames per second and saved in .tiff files. These .tiff files were then used for image processing in MATLAB. To achieve a set of streaks where the beads passed by, the difference between two images was taken, after which this was made into a new picture. This picture was then added to the next difference image, and so forth. The background noise was filtered out of each individual difference image. The final composite picture was normalized and an overlay was made of this image with one more, to add the outline of the chip to the picture. The MATLAB script used for these operations can be found in the appendix.

The background noise was filtered out by setting a threshold. This is necessary because the amount of noise in one image is significant, as can be seen in figure 10. This threshold was found by looking at the intensity plot of one difference image (not normalized), as can be seen in figure 11. The peaks represent the difference between the position of a bead in the first image and its position in the second image. It can be seen that until around 15 in intensity, there is a significant amount of background noise. When this is not removed in each image, data will be lost in the final image.
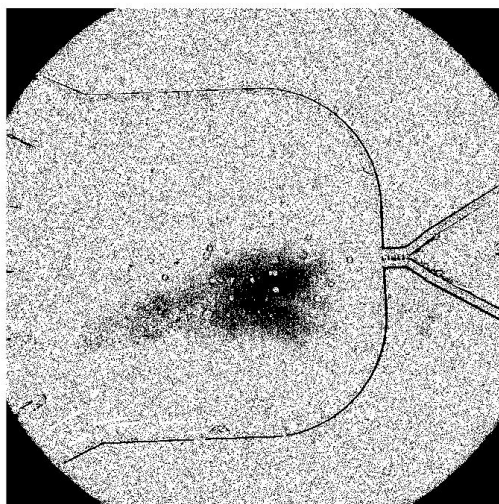
Figure 10: Difference image of two frames with a substantial amount of noise.

To effectively remove this, every pixel with a value above the intensity of 15 will be allowed to keep its value while every pixel under that threshold will be made black. This results in figure 12 after normalization, which will then be added to the next figure that is made in the same way.

The result is an image as seen in figure 13a. Figure 13b shows the end result that is achieved after overlaying 3a with one more image.

Figure 11: 3D intensity plot of the difference between two images. The peaks show the difference between the two positions of the beads.
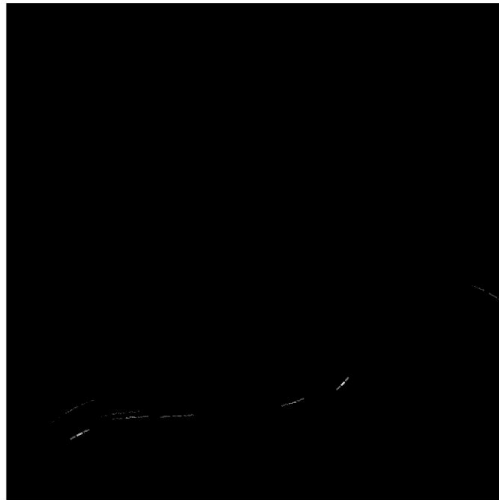
Figure 12: Normalized image after the noise is removed.

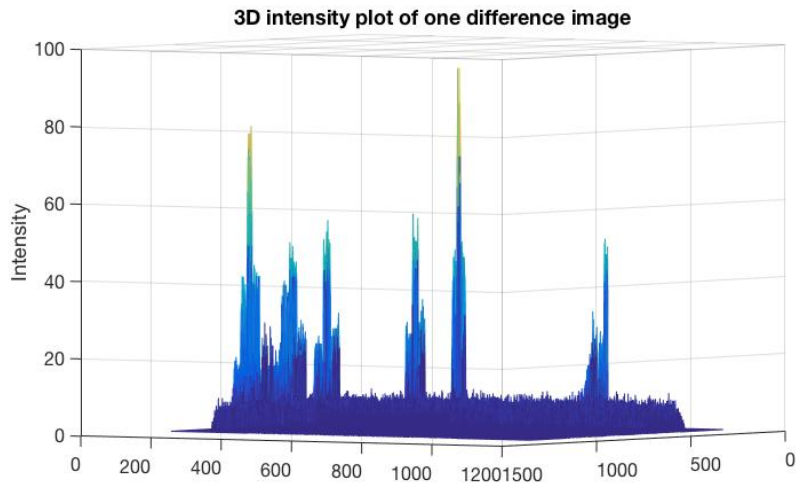Some streaks are dotted, meaning that either the particles moved the distance of their diameter in between two pictures, creating gaps, or the threshold is too high, meaning that some data is thrown away with the noise. To find the optimal threshold for each video that needed to be processed, the intensity plot as seen in figure 11 was made before processing all of the images. From this the new threshold was taken, but some data will always be lost because otherwise not all of the noise is removed.

Particle identification

The same recordings can be used to do particle identification. Using this, a histogram could be made which allows for quantitative comparison of the results. These histograms are made by the MATLAB script that can be found in the appendix (A.2). First the program searches for circles in each individual frame of the recording. The x- and y-coordinates of the centres of these circles are then all plotted in the same figure, leading to an image that shows the path of the beads (see figure 14).
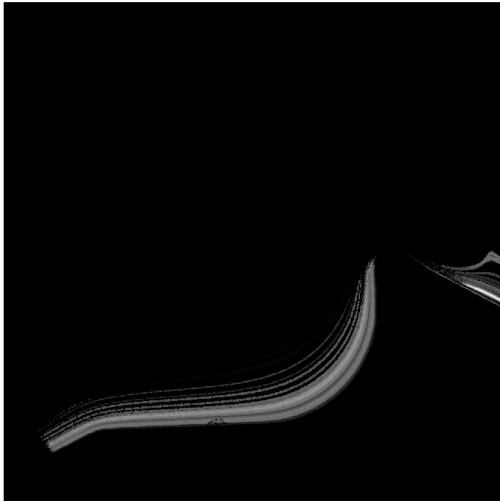
(a) The image achieved after all the difference images are added.
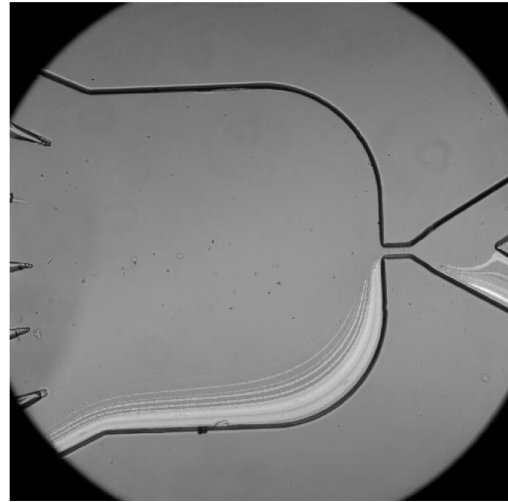
(b) The end result after the overlay is made of a and one more image.

Figure 13: Both pictures are from a measurement with 6 μm beads, with a flow rate of 200 μL per hour for the bead solution and 1600 for the buffer solution.

To make the histograms, only a vertical slice of this picture was taken at the beginning. This slice was taken to be 50 pixels wide to make sure that the program could find all of the passing beads. The slice was taken somewhere close to the outlet channels for each recording, because that is the place where, if the outlet channels are placed correctly, the beads would be separated. In the optimal situation, the beads would be completely separated just before the outlet channels. Their distribution before that point is not of importance because there they do not yet have to move into their designated channel.

Sometimes the slice had to be moved slightly because a bead was stuck in that part, meaning that the program counts it in each frame and it shows up in the histogram as a bin with an enormous amount of beads.

The histograms are simply made by the corresponding command in MATLAB. The y-coordinates of the found circles were used for all of the histograms since the slice is made vertically. The histogram divides the slice into a number of bins (in this case found to be 100 by trial and error) and counts how many y-coordinates of the circles fall in that bin. To avoid the beads falling half in one bin and half in the other the program decides for itself where to place the bins, which is why the bins in the two histograms do not completely overlap. This process is done by the automatic binning algorithm of MATLAB. [14]

When the program counts the number of beads in the slice, one bead is counted as many times as it is present in that slice in that frame. This means that all of the histograms are relative. The number of beads should be divided by the amount of times each individual bead is counted, but since this differs slightly for each bead and it is difficult to fix this, the graphs are kept with the total counts.

Since comparing histograms by eye is subjective, the need arose for a number that could provide quantification of the results. This could improve the support for any possible claims made in the conclusions. Keeping in mind that the end goal of the device is to count individual parasite eggs so that it can be decided whether or not the horse is infected with worms, it is undesirable to have the different eggs mixed together. Especially since different kinds of eggs require different kinds of antibiotics. Because of this, it was reasoned that it would be the most useful to have a number that represented the amount of beads that, when the outlet channels would be put at exactly the right place, would be 'pure' in their outlet channel. This means that in a histogram, the blue
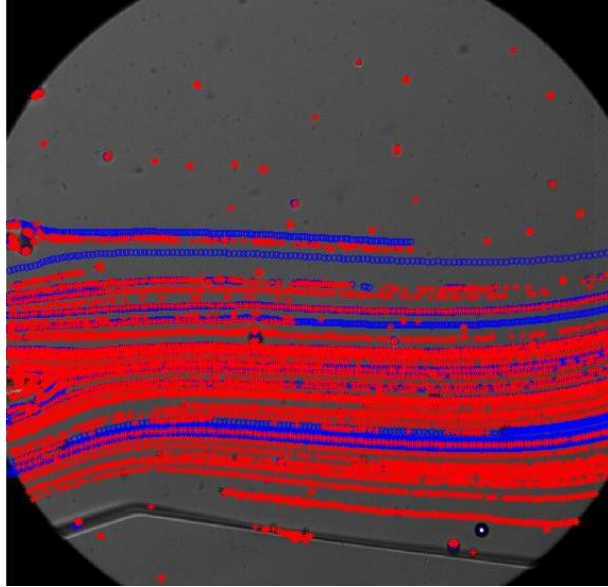
16

Figure 14: Particles identified and plotted together to show the path of the beads. Red stars are the 6 μm beads and the blue circles are the 20 μm beads. The outside of the chip is below and the first outlet channel in the lower left corner. This image was made with the ratio of 1:3.

bins for example at the left side of the axis that have no red bins on the same spot are taken into account as 'pure'. The amount of beads these blue bins represent divided by the amount of total beads of that size found in that measurement would then result in the percentage of beads (of that size) that could theoretically be completely separated without any contamination of the other size beads. For the 6 micrometer beads the same holds, only the 'pure' beads are then the bins at the right side of the axis without any blue bins disturbing their spot. This percentage was called the percentage of separated particles (or PSP) for easy reference. Following this calculation, a 100% PSP would mean that all of the beads are separated (which is the optimal situation) and a 0% PSP means that at least for that size beads, there is no separation from the other size.

Instead of the method described above, also the amount of overlap could have been looked at. Quantifying this would have resulted in a percentage that represents the amount of beads that are mixed. This would say the opposite of the PSP as mentioned above, a 100% score would mean that all of the beads were overlapping. This was found to be less useful, since the number of not-mixed beads was desired and quantifying the overlap would then require an extra operation to get that percentage.

5 Results

In this section the results from the experiment of both separation and detection will be shown. This also includes the artefacts, or observed obstacles, that occurred during the tests.

5.1 Artefacts

During the experiments several problems occurred. This section will elaborate on the different kind of problems that were encountered and the methods used to solve them.

The most common problem that was dealt with was air bubbles. Each time the chip was flushed through with water first, some air bubbles were left in the outlet tubes and sometimes in the channels in the chip. Before any experiments could be performed, these bubbles had to be removed because they change the resistance of the outlets. To get a correct separation, the resistance in each channel has to be the same otherwise the separated particles might still proceed into the same channel. Bubbles as the one seen in figure 15 have an effect not only on the channel the particles end up in, but also the separation set in motion by the pinched segment. This because less volume of solution can pass by at that point, leading to a disturbed distribution of flow.

To remove all of the bubbles from the chip, more pressure had to be exerted so the water was flushed through at a higher flow rate (6000 $\mu L/hour$).

If that didn't remove the bubbles, a set of tweezers was used to - while still flowing the water - apply even more pressure to the individual bubbles by pressing down on the chip at their location. Since there were most of the time also air bubbles in the outlet tubes, another method had to be thought of to remove those too. The method that eventually worked best for the bubbles in the chip and in the outlet tubes was the following: all of the outlet tubes were pinched except for the one the bubble was located in. This last tube was pinched shortly, building up the pressure (the water was kept flowing) and then released suddenly. As a result, the bubble shoots through the tube to the end.

This method is efficient for bigger bubbles, however small ones that do not occupy the width of the channel do not respond as well. To remove these a combination of building up pressure and using the tweezers to narrow the channel next to the bubble was used. In this way the water was forced to flow along the channel side blocked by the bubble, resulting in the water pushing the bubble forwards. Encountering a lot of trouble with the air bubbles it was decided to make a charge of new chips. These chips were bonded to the glass plate, so treated in the plasma oven, but not put into the oven afterwards. The last step was done the first time to further strengthen the bonding, but makes the chip also less hydrophilic. So without it the chips are more hydrophilic, which makes it easier to remove the bubbles.
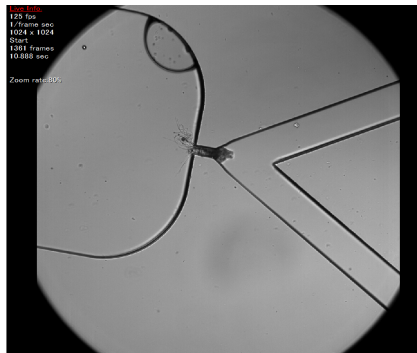

Figure 15: A piece of PDMS stuck in the pinched segment and an air bubble in the broad segment.
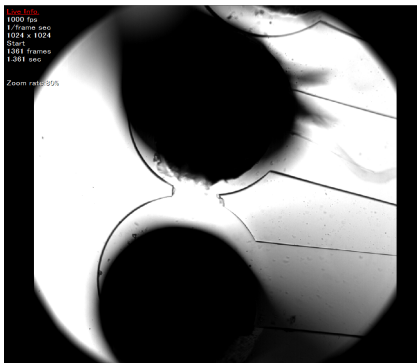

Figure 16: Two outlets merged together.

Figure 17: Failed bonding, beads end up outside of the channels.

The new chips were a lot more hydrophilic than the old ones which decreased the problem with bubbles significantly. At the same time it also caused a new problem. It seemed that the beads are hydrophilic and therefore, like to stick to the surface. When too many beads stuck in the broadening segment after the pinched segment the sorting was influenced, by the beads blocking the way or working as an obstacle causing the streamlines to change and consequently the pathways of the beads were altered. This problem was removed by building up pressure and realising it one after another to each of the outlet channels. Applying higher buffer solution flow rates sometimes helped as well, in extreme case the syringe needed to be pushed manually to get a high enough pressure.

Figure 15 also shows another problem that sometimes occurred, pieces of PDMS that get stuck in the pinched segment. This often happened after several experiments were performed or when the tubes stuck in the inlets were moved, for example when mixing the bead solution. The solution to this was applying pressure until the piece shot through the pinched segment, after which it is removed via the outlets. This pressure was either applied by pushing down on the pinched segment with tweezers while flowing the water at 6000 μL per hour or, if that didn't work, taking the water syringe out and applying pressure by hand.

Some less common problems were for example fused outlets (figure 16) or failed bonding (figure 17). Fused outlets means that something in the lithography went wrong, it could be that there was still some SU-8 left on the spot between the two outlets, leading to the PDMS creating a channel there. Perhaps the development was too short, so that not all of the SU-8 was washed off.

Figure 18: Three beads of 6 micrometers, two are significantly faster than the third, as can be seen by the shape.

Failed bonding means that the PDMS chip is not bonded to the glass plate well, leading to leakages and an unusable chip. Bonding can fail when the chip is not left in the plasma oven long enough, or there was too much time in between taking it out of the oven and putting the chip on the glass. It can also be caused by too much or a too large piece of dust sitting in between the PDMS and glass.

In figure 18 it can be seen that two beads of 6 micrometers are moving at a significantly faster pace than the third one in the picture. In the image, the two beads are streaks, while the slow bead is - like they appear when standing still - round. Since the two fast beads are on each side of the slow one, the logical explanation would be that the slow-moving bead is located more at the bottom of the chip. The flow profile in the chip, since it is laminar flow, is parabolic over the width of the channel, but also over the height. The beads tend to sink in the syringe, leading to the assumption that they also sink inside the channels in the chip. This sinking would leave them in the lower part of the flow profile where the velocity is lower.

Figure 19: A set of 6 μm beads stuck together and a set of 20 μm beads stuck together.

Sometimes it occurs that several beads go through the pinched segment at once, because they are stuck together (see figure 19). This results in broader streaks, but while that should in theory make the separation worse, it was observed that when 20 micrometer beads stuck together they proceeded into the right channel while single beads did not.
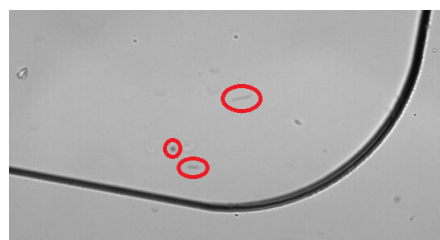
5.2 Separation

The separation of the pinched flow fractionation (PFF) was tested as described in section 4.5. Flow rates were differed as well as the ratio between the flow rate of the buffer and that of the bead solution to investigate the effect on the efficiency of the separation.

Ratios and flow rates

According to the theory, the ratio between the flow rate of the beads solution and the buffer solution has a significant effect on the separation of the particles. This because with a higher ratio, the buffer flows faster and the beads get pushed more to the wall. This creates a bigger difference between the small and big beads which leads to them ending up in a more different range in the broadening segment. In this section the results of the experiments testing this theory are presented. It will also be investigated whether or not the magnitude of the flow rate has an effect on the separation.

5.2.1 Design 1

Efficiency

To determine which flow ratio caused the most separation of the particles in the first design, histograms were made. By looking at the overlap of the two different beads in these histograms the efficiency of the separation can be determined. In this report, the result of the separation will be shown as the percentage of separated particles (PSP). This allows for quantitative comparisons between different ratios. Unfortunately, this method could only be applied to one design, which means that for the second design no quantitative comparisons could be made.

The first thing that was noticed during the experiments was that there were a lot of 20 micrometer beads that clotted together. Also, on the raw unprocessed footage it can be seen that these clots most of the time end up higher in the broad segment than the single beads. Unfortunately the histograms don't show this.

Figure 20 shows the results of the PSP calculation for each ratio. For the ratios with the higher flow rates (total flow rate of 1000 microliter per hour), the ratios 1:7 and 1:9 seem to have the highest PSPs. From 1:9 on the percentage gets lower and the overlap between the two different beads bigger. This is also visible in the histograms shown in figures 22 to 28. For the lower flow rates (measured in a different chip) the ratio of 1:6 gives a similar result as 1:7. The measurement of the higher ratio 1:10 only captured two 20 micrometer beads, which leaves uncertainty on how more would behave. At the ratio of 1:20, a 100% PSP was found for both the 6 and the 20 micrometer beads, as the 20 micrometer beads were very concentrated.

The different PSPs make something else prominent, namely that the percentage for the 20 micrometer beads is always lower than for the 6. This is also seen in the histograms, mostly there are some 6 micrometer beads that appear in the range of the 20 micrometer beads while the 20 micrometer beads stay away from the bulk of the 6s.
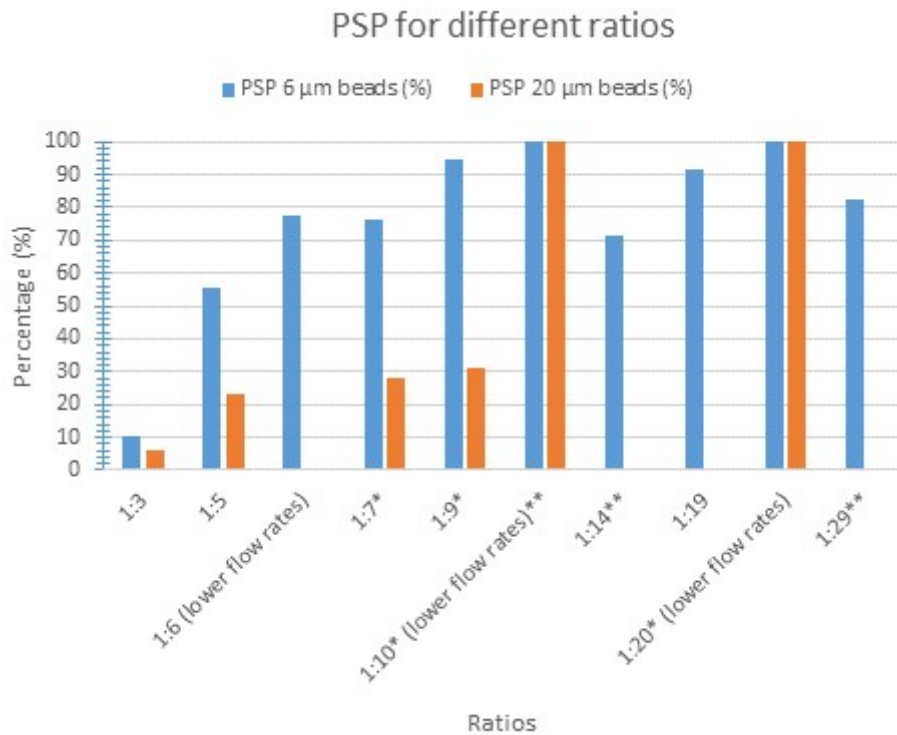
Figure 20: Different ratios and the corresponding percentages of separated particles (with a high probability for errors in 1:10, 1:14 and 1:29)

Some bins were not taken into account when calculating the PSP, since the number of beads in this bin was very small compared to the other bins.
*** Some ratios had a very few amount of beads passing, had there been more beads the PSP might have been different. The ratio 1:10 had two 20 micron beads passing by, 1:14 had two 20 micron beads passing and 1:29 had three 20 micron beads passing.*

Several things can be noticed immediately when looking at the histograms. Firstly, in each histogram there are peaks below the amount of times one bead is generally counted. This would mean that these peaks indicate less than one bead passing by. It is more likely that either the bead is moving faster than the others and is therefore counted less times, or the program found beads where there were none. For some calculations of the PSP, these bins were not taken into account when the number of counts in that bin was significantly less than the number of counts in the other bins that corresponded to one bead and taking it into account would have a big impact on the PSP. To verify that these bins are actually not beads passing by, the raw footage was called upon and for the two counts at 630 pixels at the ratio of 1:7 for example, it was checked. This was also done for the one at the ratio of 1:20.

Furthermore, the decrease in the number of beads passing by is significant. At some of the high ratios, very few beads passed by during the measurement. This holds for the ratios of 1:10, 1:14 and 1:29.

Figure 21a shows where the different beads passed by at the ratio of 1:3. Figure 21b shows the path of the beads at the ratio of 1:9 throughout the measurement. The red crosses are the 6 micrometer beads and the blue circles are the 20 micrometer beads. Figure b shows that most of the 6 micrometer beads are indeed concentrated in a different range than the blue 20 micrometer beads, although several 6s followed the same path. This is a stark contrast to the overlap seen at a ratio of 1:3. It can also be seen in the figures that the program finds some beads where they are not.

Figure 22 shows the results of the histogram of the lowest ratio tested (1:3). It can be seen that the 6 and 20 micrometer beads have a large overlap and at around 730-750 pixels the 20 micrometer beads are even fairly dominant.
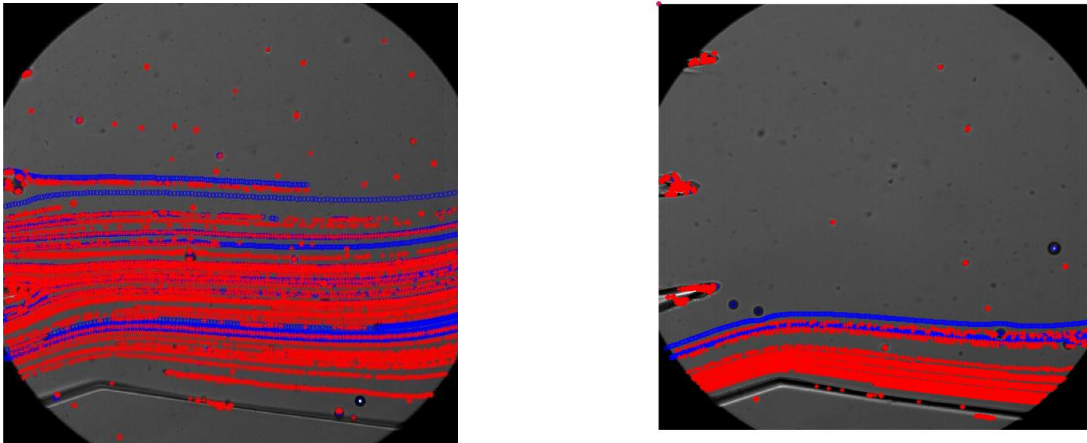
(a) The path followed by the beads at a ratio of 1:3.

(b) The path followed by the beads at a ratio of 1:9.

Figure 21: Particle identification for a complete recording of ratios 1:3 (a) and 1:9 (b).
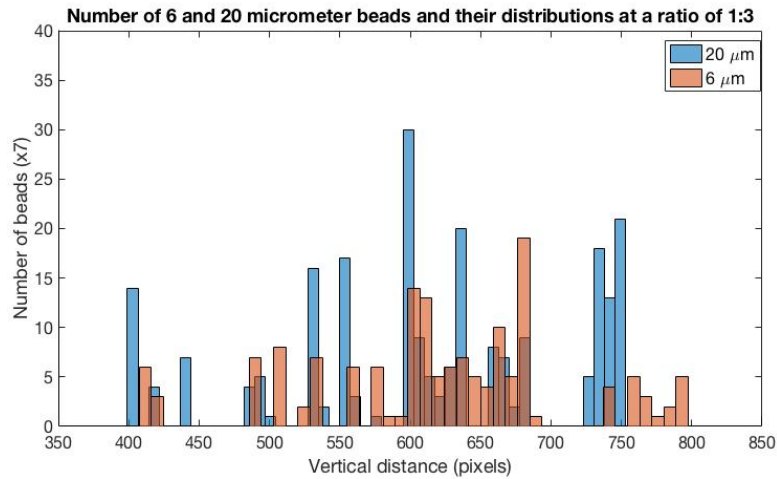
Figure 22: Histogram of the ratio 1:3. PSP6 = 10.3%, PSP20 = 6.1%

In figure 23 already some improvement can be seen, as the overlap is much less significant and the range of primarily the 6 micrometer beads has become much smaller. It has also moved more to the right of the axis. There is however still significant overlap and the PSPs of both beads is not very high. For the 20 micrometer beads this is mostly caused by the 6 micrometer bead at around 370 pixels. This peak is peculiar as the rest of the 6 micrometer beads don't come below 680 pixels. Also, there are only seven counts in this bin, whereas most beads were counted 12 times. This could be a mistake of the program or a fast moving, wrongly separated bead. Without that bin, the PSP of the 20 micrometer beads would increase significantly to at least 38% When looking at the raw footage of the measurement, a 6 micrometer bead did indeed pass by in that range, meaning that the program was right.

Apart from the appearance of a 6 micrometer bead at 370 pixels, the broad range of the 20 micrometer beads can be noticed. The beads are not nearly as concentrated as the 6's seem to be. Not only that, but it is peculiar that there are completely empty ranges in between the blue bins.

22
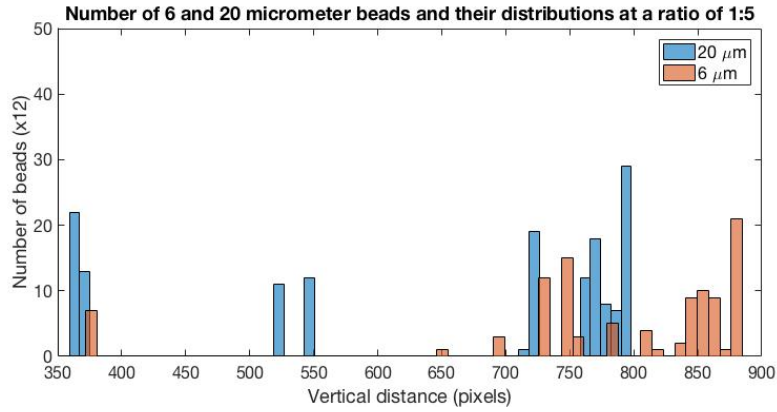
Figure 23: Histogram of the ratio 1:5. PSP6 = 55.3%, PSP20 = 23.0%

The ratio of 1:7 did clearly improve the separation with respect to 1:5 for the higher flow rates as both of the PSPs increased. When looking at the histogram (figure 24), it can be seen that the 6 micrometer beads occupy a somewhat smaller range than seen at a ratio of 1:5. The 20 micrometer beads seem to have a smaller range and one bead is an outlier here. What is most important is that the overlap is much smaller, the only significant overlap is at around 750 pixels.

The PSP of the 20 micrometer beads would have been higher without the red bin at 685 pixels. A look at the raw footage showed that there were no single 6 micrometer beads passing by at 680 pixels, but there were several clotted beads.
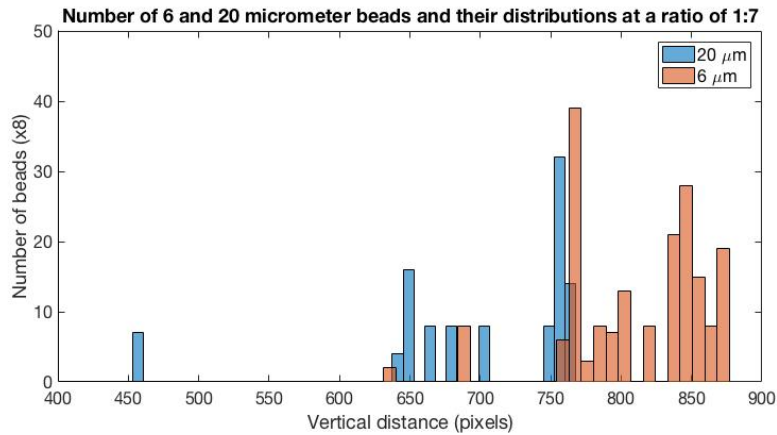
Figure 24: Histogram of the ratio 1:7. PSP6 = 76.5%, PSP20 = 28.1%

The ratio of 1:6 results in a similar PSP6 as the 1:7, but the PSP for the 20 micrometer beads is 0% because there is one bead that passes by above the last 20. The figure can be consulted in the appendix (A.1).

At a higher ratio of 1:9, the ranges of both bead sizes get smaller still and the bulk of both is concentrated more on the right of the graph (see figure 25). As with the other ratios, several 6 micrometer beads cross over into the range of the 20 micrometer beads which leaves the latter with a low PSP.

When comparing this ratio with the 1:7, one other thing spikes interest. The distance between the bulk of the two sizes of beads is larger at the ratio of 1:9 as with the 1:7 there is no distance in between. This trend is continued by the ratio of 1:19, where there is also a fair distance between the bulks. The ratio of 1:14 does not follow this trend.

There is a significant difference between the ratio of 1:9 and the ratio of 1:10 in the other chip, namely that the range of the 6 micrometer beads at 1:10 is a fair amount larger than at 1:9, and the 20 micrometer beads are found more to the left of the graph (further away from the channel wall). Also, the distance between the two bulks in 1:10 is almost non-existent like the ratio of 1:7.
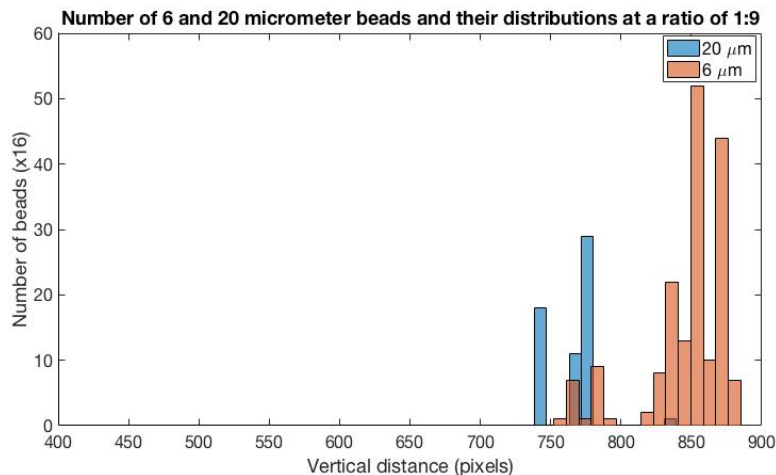
Figure 25: Histogram of the ratio 1:9. PSP6 = 94.9%, PSP20 = 31.0%

The ratio of 1:14 shows a range of the 6 micrometer beads much like the ratio of 1:10, about the range of the 20 micrometer beads, like at the ratio of 1:10, not much can be said since there were so little. The graphs for these two ratios can be found in the appendix (A.1).

After the ratio of 1:14, 1:19 shows a much larger amount of beads, and with it comes a smaller range of the 6 micrometer beads if one does not take the few outliers into account. Much like with 1:9, the bulk of the beads is between 800 and 900 pixels. However it seems that the 20 micrometer beads are less concentrated on the same spot than at the ratio of 1:9. The PSP20 is 0% because of the outliers of the 6s, but the PSP6 is very high (91.3%).
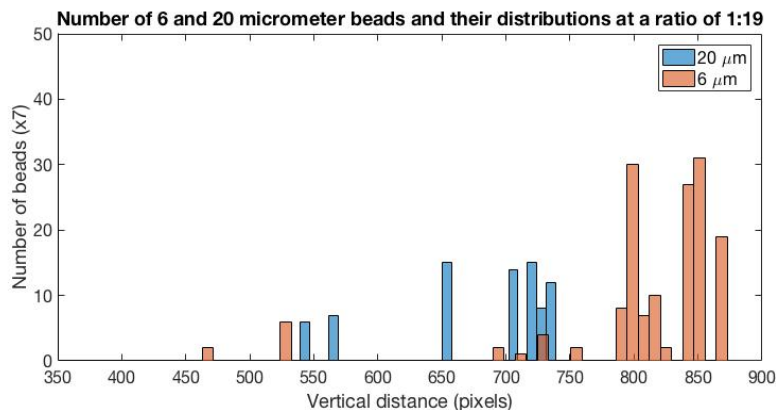
Figure 26: Histogram of the ratio 1:19.
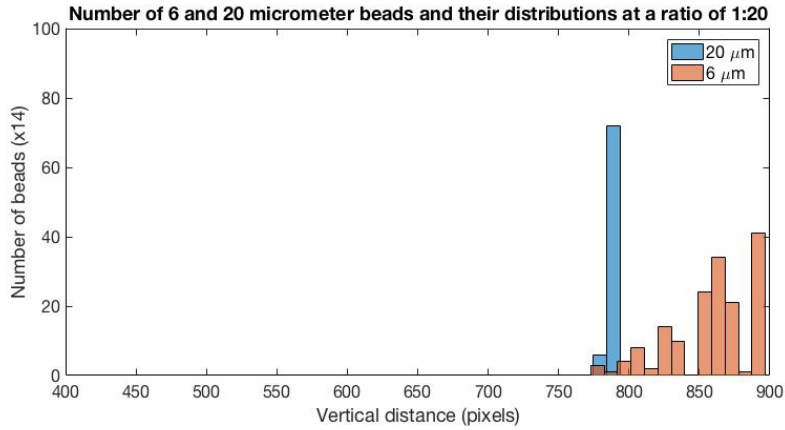
Figure 27: Histogram of the ratio 1:20

When comparing the ratio of 1:19 with the ratio of 1:20 tested with the other chip, the PSP6 seems to match, but the range for the 20 micrometer beads does not (figure 26 and 27). The 20 micrometer beads at 1:20 are much more concentrated than at 1:19, with 5 beads following almost the same path. The distance between the bulk of the 6s and the bulk of the 20s however is much larger for the 1:19 ratio.

The last ratio that was tested is seen in figure 28. This figure shows the ratio of 1:29. The separation seems very good, although there is one 6 micrometer bead in the range of the 20s. However the distance between the bulk of the 6s and the 20s is bigger, like at 1:7 and 1:19.
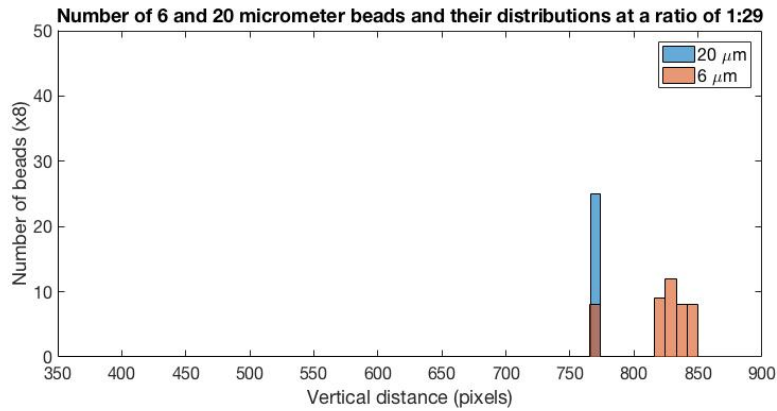
Figure 28: Histogram of the ratio 1:29

5.2.2 Design 2

In the following results of the experiments with the second variation of this design testing the above mentioned theory are presented. The first variation turned out to have the outlets too close to each other to pinch the holes for the outlet and/or put outlet tubes inside without causing any ruptures. The ruptures led to leakage and made the chips unusable.

Flow rate ratio

In literature ratios of 1:50 [15] are used for the asymmetric pinch flow. Therefore, the same ratios as before were tested, but also higher ratios, to investigate the influence of them. Several total flow rates were investigated for this design. A total flow rate of 2000 μL/h seemed to be the best, as the flow rate for the 20 μm beads with high ratios became too slow otherwise. Consequently a

fixed total flow rate of 2000 μL/h was applied in the experiments.

Figure 29 shows the intensity plots of the 6 μm and 20 μm beads for the different ratios tested and with a total flow rate of 2000 μL/h.

The brightest streaks represent the path that the most beads followed, since all of the pixels where beads were kept their intensity value. Each time another bead passes by, the intensity value of that pixel becomes higher.

With a ratio of 1:5 (figure 29a) the beads ended up relatively random in the first three channels. The streaklines of the two different beads overlap each other two much as that each of their path could be tracked. The 1:7 ratio (figure 29b) shows a separation of the two beads, but both flow into the first channel. The same accounts for the 1:9 ratio (figure 29c) with the only difference that the streaklines overlap more, possibly because of an high total amount of 6 μm beads passing by. Increasing the ratio further to 1:19 (figure 29d) a clear differentiation between the two beads cannot be made. Looking at the video itself, one sees clusters of two larger beads flowing into the second channel, but single 20 μm beads flowing into the first channel. The single 20 μm beads took a similar pathway compared to the 1:9 ratio. The smaller beads all flow into the first channel. All beads ended up in the first channel again with even higher ratios. A slight separation of streaklines can be seen for both the 1:39 ratio (figure 29e) and the 1:60 ratio (figure 29f). The range covered by the beads seem to decrease.

Comparing all streakline images the beads turning midway into the first channel stand out. This can be seen best in figure 29b and figure 29c, where the 20 μm beads are first clearly separated and then turned shortly before arriving at the channels to the right and flowed into the first channel. During the experiments this was also observed for the second channel. Furthermore, it came to notice that no mayor flow came out of the draining channel tube. Due to a lack of time this could not be further investigated. In the discussion more is said about these phenomena.
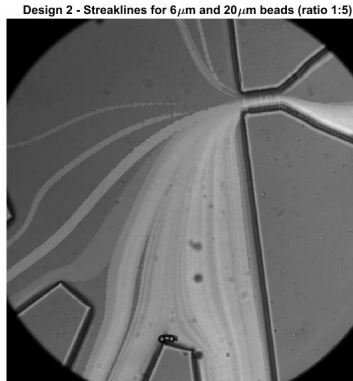
(a) Streakline image of both beads at ratio 1:5
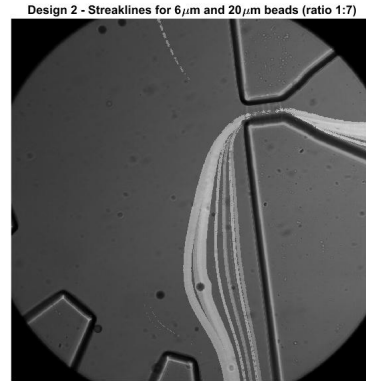
(b) Streakline image of both beads at ratio 1:7
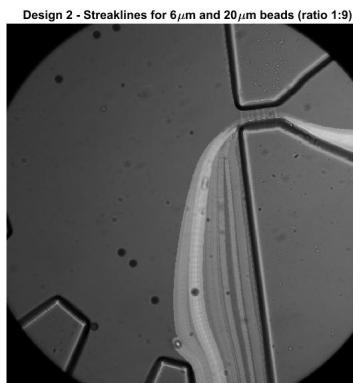
(c) Streakline image of both beads at ratio 1:9
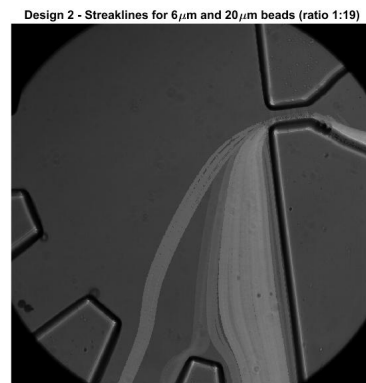
(d) Streakline image of both beads at ratio 1:19
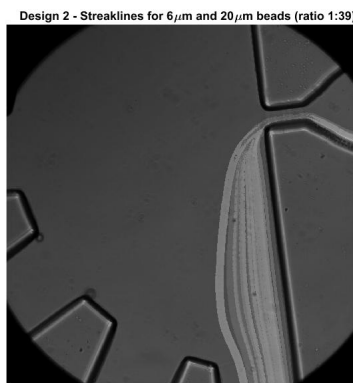
(e) Streakline image of both beads at ratio 1:39
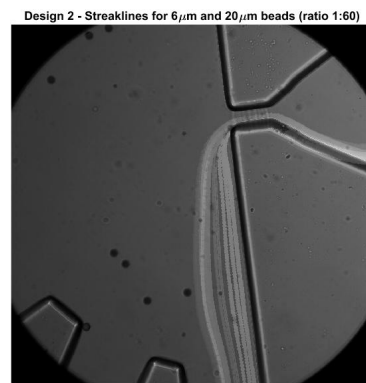
(f) Streakline image of both beads at ratio 1:60

Figure 29: Streaklines for the 6 μm and 20 μm beads for the different ratios tested with the asymmetric pinched flow design, variation 2

Efficiency analysis

An analysis of the efficiency with the Matlab program requires a certain magnification. The 6 μm beads need to have a size of at least one pixel, which was not the case for the recordings made. Therefore, the efficiency analysis could not be made for the second design.

5.3 Concentration

The concentration was assessed by taking 10μm of the solution in the syringe and the same amount of fluid from all outlet tubes with the chip running. These samples were investigated by an auto-

matic cell counter first. This would have been the most time saving method, but did only work for the 20 μm beads and not for the 6 μm beads. For the outlet solution no beads were found at all. Encountering this problem, the beads were counted under the microscope with the help of a cell counting device. This cell counting devise is usually used to count blood cells, but as these cells are in the same order of magnitude with regard to their size, it can also be used to count beads. As the distribution of beads appeared to be uniform and there was a lack of time, the beads in only one of the nine squares (containing sixth-teen squares itself) were counted. For the cell counter Bücker used the following equation [16]:

$$Particles\ per\ \mu L\ volume = \frac{Counted\ Particles}{Counted\ Surface\ (mm^2) * Chamber\ depth(mm) * Dilution}$$

Table 3: Counting of beads and resulting concentrations (in beads/μL) of the different beads in the two solutions used, as well, as the calculated concentrations (in beads/μL).

beads	20 μm 1st solution	6 μm 1st solution	20 μm 2nd solution	6 μm 2nd solution
counting	44	61	124	295
concentration	-	-	4650	303850
calculated concentration	4600	4600	2270.4	2270.4

In the table above, the 1st solution has an unknown dilution value, so the final concentration could not be calculated.

5.4   Filtration

Due to a lack of time the hydrodynamic filtration could not be tested. Apart from that, it seemed that the small channels were designed too small to survive the fabrication process. The channels were either not present at all, or partly collapsed. The first could be because of a too short development during the fabrication and the second because of capillary forces inducing too much stress on the walls while drying the wafer with the SU-8 after the development. Latter might be prevented by decreasing the height of the chip.

5.5   Detection

The first measurements obtained from the initial set up are shown in the table 4. The results show that the detection is not working sufficiently because in some cases the current value is higher, in higher concentrations. That was expected since the area of channel was extremely small with respect to the area that the photoresistor was sensing. Furthermore, the light intensity was spread in a larger area and not focused on the channel which makes the sensing less accurate. Last but not least, reflections from the chip and the glass are also contributing to a lower accuracy of sensing the particles.

Table 4: Measurements with the initial set up.

Concentration (beads/ul)	Chip	Channel (mA)	Temperature before	Temperature after
Only air	none	11.544	22.8	22.8
Glass plate	none	10.705	23.2	23.4
Empty channel	1	11.394	23.6	23.6
Empty channel	2	11.45	23.6	23.6
Empty channel	3	11.948	23.6	23.6
Demi-water	1	11.294	23.4	23.4
Demi-water	2	11.296	22.8	22.8
Demi-water	3	11.31	22.8	22.8
1825	1	11.3632	22.8	22.8
1825	2	11.512	22.8	22.8
1825	3	11.013	22.4	22.6

After those improvements new measurements where done. As it can be seen in table 5 the current value has dropped at approximately 35% of the original value. That drop was expected since the sensor is now focused only on the light intensity passing through the channel. The results here show, that the system now can detect more accurately the difference in the concentrations.

Table 5: Measurements for the improved set up.

Concentration (beads/ul)	Channel 1 (mA)	Channel 2 (mA)	Temperature before	Temperature after
Empty channel	3.911	3.917	22.6	22.6
Demi-Water	3.88	3.895	22.6	22.8
1825	3.84	3.812	22.8	22.8
912.5	3.831	3.78	23	23
Demi-water	3.853	3.818	22.8	23
1825	3.806	3.796	23	23
912.5	3.812	3.785	23	23

New measurements where taken by using the tube as channel and the results can be seen in the table 6. From the data it is visible that the detection accuracy has been increased even more. Key factor to that are, the constant temperature during the measurements and the larger height of the channel.

Table 6: Measurements using a tube instead of a chip.

Concentration (beads/ul)	Channel (mA)	Temperature before	Temperature after
Demi-water	3.894	23.8	24
912.5	3.831	24	24
1825	3.745	24	24
Demi-water	3.864	24	24
912.5	3.824	24	24
1825	3.728	24	24

Observing that the temperature is constant on the data of table 6, gives the possibility to plot a calibration curve. That can be seen in the figure 30. That is done by taking the average output current value for each concentration.
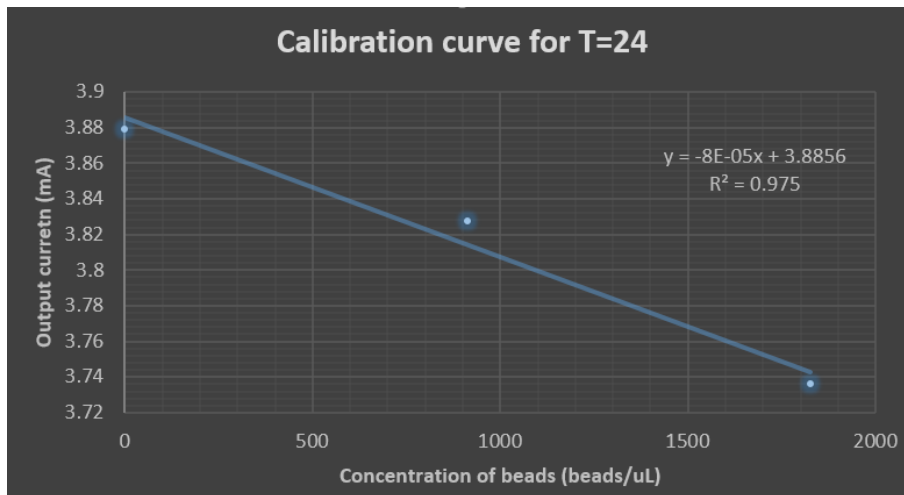
Figure 30: The calibration curve for a temperature of 24 degrees Celsius.

During the measurements the cone on the top of photoresistor had to be replaced. That cone was made by hands and it was very difficult to duplicate it. So, the diameter of the new cone is different. New measurements are performed and the results can be seen in table 7. From the new value of the current it can be concluded that the diameter value in the second cone was smaller. Next step would be to take the average of each concentration from the table 7 and make a calibration curve(like it is done for table 6) but in this case the temperature has an impact on the system, so it can not be neglected. Thus, the data are presented in the above tables instead.

Table 7: Measurements using a tube instead of a chip, after replacing the cone.

Concentration (beads/ul)	Channel (mA)	Temperature before	Temperature after
Demi-water	2.078	22.8	22.8
365	2.212	22.8	22.8
456.25	2.089	22.8	22.8
602.25	2.082	23	23
912.5	2.076	23	23
1825	2.076	23	23
Demi-water	2.098	22.8	22.8
365	2.044	22.8	22.8
456.25	2.095	22.8	22.8
602.25	2.034	22.8	22.8
912.5	2.041	22.8	22.8
1825	2.02	22.8	22.8
Demi-water	2.832	22.6	22.6
365	2.447	22.6	22.6
456.25	2.241	22.6	22.4
602.25	2.384	22.6	22.6
912.5	2.382	22.4	22.4
1368.8	2.854	22.4	22.4
1642.5	3.315	22.2	22.2
1825	2.854	22.2	22.4

6 Discussion

6.1 Artefacts

Several times during the experiments, pieces of PDMS got stuck in the pinched segment of the chips. This greatly affected the working of the chip and measurements could not be done until, if possible, the piece was removed. An explanation for these appearing pieces could be that the holes for the inlets were punched too roughly, leaving pieces of PDMS slightly loose. After the water or bead solution is pushed past a couple of times, the pieces get completely loose and continued down the channel to then get stuck in the pinched segment.

A common occurrence was beads sticking together. Since this affects the separation (as PFF works based on size), this was a problem. For the beads sticking to the walls of the syringe and the tubes and the channels in the chips, the solution was to put Tween into the suspension. This worked, but even afterwards clusters of beads would still appear in the footage. The reason for the beads sticking together might be that they were pressed together in the syringe. Since all of the beads tend to sink, the weight of the beads might have compressed a few and created the clusters. Another reason could be that the beads are attracted to each other and thus stick together, but the amount of clusters would (presumably) have been much higher in that case.

Making new chips without putting them in the oven after the bonding proved to be very helpful when facing problems with air bubbles inside the tubes and the chip, as it left the chip hydrophilic. However, the beads seem to stuck more to the surface of the chip, suggesting that they are hydrophilic themselves. Taking high enough flow rates, this problem could be prevented.

Fixing the total flow rate rather than one of the flow rates, of either the bead or buffer solution, turned out to be the best way to compare different ratios and at the same time prevent the beads from sticking before or after the pinched segment. The total flow rate had to be chosen high enough to guarantee the latter, but not so high as to create vortices after the pinched segment.

6.2 Separation

6.2.1 Separation in general

The syringe itself can be sticky with regard to its smoothness in pushing the beads out. This stickiness causes noise. As long as the flow rate is high this noise is relatively low and will not have any significant effect on the separation of the beads. If the flow rates ,however, drop, the noise becomes relatively bigger and will eventually influence the sorting. This influence will manifest in beads flowing less straight towards their destination. So when dealing with very slow flow rates this can affect the sorting and thus was one of the reasons why total flow rates of 1000 μL/h and 2000 μL/h were chosen, to keep the individual flow rates from getting too small.
The pump itself can cause the same kind of noise, especially for slower flow rates. This problem is most likely due to the motor of the pump itself. In the beginning of the experiments the pump and syringe used, both caused so much noise that literal "bead explosions" could be observed. After replacing pump and syringe this phenomenon was not observed any more.

Making new chips without putting them in the oven after the bonding proved to be very helpful when facing problems with air bubbles inside the tubes and the chip.

6.2.2 Design 1: PFF

The histograms proved a useful tool for a quantitative analysis.The percentage of separated particles that could be acquired based on these graphs shed light on the results of the different flow ratios. These PSPs made it clear that low ratios (in the range of 1:3 and 1:5) do not have a positive effect on the separation. At these ratios the particles can end up in a large range across the broadening segment. It is also shown that with increasing ratio, the percentage increases as well. Based on the percentage, the range which the beads are found in and the distance between the two ranges the ratios of 1:9 and 1:20 seem to provide the best results, although it is unclear why their corresponding ratios at respectively lower and higher flow rate magnitudes are so different. To investigate which of these ratios, if one of them at all, is the optimum for the separation, more measurements would have to be done.

It should be clear that the PSP is not completely accurate, since not all of the beads are counted as many times as others for example because they're moving faster than average. As a result, these beads count for less than one while they actually should count for one. However, since the reason they're counted less is unknown, it is not possible to count them as one as they could also be faults of the program. The same, though inverted, goes for the beads that are counted more times than the average.

Looking at the results of the first design, it should be noted that at 1:14 and 1:29 so little beads passed by that the resulting PSPs are disputable. That so little beads passed by could be caused by the low flow rate of the bead solution at those ratios (66.7 and 33.3 microliters per hour respectively). At this flow rate the beads might have more time to sink, leading to less beads reaching the chip. However, at 1:10 and 1:20 more beads were visible during the measurement, even though the flow rate of the bead solution was even lower (20 microliters per hour for both). This leads to the assumption that the low flow rate was not the cause of the shortage of beads. A lot of other parameters could have caused this, such as the beads in the syringe not being mixed before taking the measurements or the beads sticking to that chip more than the one the 1:10 and 1:20 measurements were taken with. It's hard to determine the cause afterwards, if more measurements had been done perhaps the answer would have presented itself.

In several histograms some bins contained a number of beads that one wouldn't expect when looking at the rest of the distribution of those beads. For example in figure R.2, a bin at around 370 pixels contained seven counts of a 6 micrometer bead, which has a big impact on the PSP of the 20 micrometer beads. In this case, the program was right but there were other bins that contained counts where no bead had passed by. Since the overall number of beads passing by was not fairly high, it is hard to say whether or not beads like the one in figure R.2 would be a common occurrence at that ratio. The question could maybe have been answered had there been more recordings

of the same ratios.

It occurred more than once that one or several 6 micrometer beads were far away from the bulk, while it almost never occurred for the 20 micrometer beads. There are several possible explanations for that, the first is that the separation simply doesn't work well enough and once in a while a small bead gets caught in the wrong part of the flow profile. Another explanation can be that while in the pinch, something obstructed the bead's path near the wall of the pinched segment. If it's not pushed against the wall completely, it will end up higher in the broadening part. This something could either be that two 6 micrometer beads were stuck together in the pinch and separated after, or it could even be stuck to a 20 micrometer bead.
These small beads ending up in the range of the 20 micrometer beads poses a significant problem. At a high concentration some beads ending up in the wrong path is not that much of a problem when counting the beads, but at the low concentrations that the parasite eggs will be present in, it will have a big impact and greatly affect the accuracy of the test.

When looking at the histograms of the ratios of 1:19 and 1:20 several differences can be distinguished. As discussed in the results, the beads are far more concentrated at the ratio of 1:20 than they are at 1:19. On the other hand there is more distance between the two sizes at 1:19. It's still not quite clear what could have caused this significant difference between the two ratios. The first thing that comes to mind is that it had something to do with the measurements being done with a different chip, but then one would expect the ratio of 1:10 to differ in the same way from 1:9 and the 1:6 from 1:5 or 1:7. But although the 1:6 is more like the 1:7 and not the 1:5, it still bears a lot of resemblance to the other ratio. The 1:10 does differ from the ratio of 1:9 but in the opposite way that 1:20 differs from 1:19. 1:10 presents a bigger range for the beads instead of a smaller one like 1:20 does. All of this does not clarify the inconsistencies. The other reason could be the magnitude of the flow rate. For the 1:6, 1:10 and 1:20 the flow rate for the bead solution was kept at 20 microliters per hour while this flow rate was higher for their corresponding ratio of the other chip. To be able to say with certainty what caused all this, more measurements would have to be done.

As mentioned in the results, table 1 displays a trend in the PSP of the 20 micrometer beads with respect to that of the 6 micrometer beads. The PSP20 is always significantly lower than the PSP6. This is something that is also shown by the histograms, there is always a 6 micrometer bead in the far range of the 20 micrometer beads, while this is very uncommon the other way around. That the 6 micrometer beads tend to stray more could be because of them not being completely pushed to the wall as mentioned in this discussion before. A higher ratio would solve this (since the area of the stream would be smaller), but even then these beads still appear in the wrong range. Only the 1:20 shows promising results. Again more measurements should be done to investigate whether or not the problem can be solved that way. The 20 micrometer beads do not stray (unless clotted together), presumably since they are always pushed to the wall because of their size. Even at the lowest ratio the area of the particle stream is smaller than the diameter of the 20 micrometer beads (the ratio would have to be less than 1:1 for the beads not to be pushed completely against the wall).

Lastly, several times when calculating the PSPs for the different ratios some bins were not taken into account. This was done if there were very few counts in the bin compared to the average number of counts that represented one bead for that measurement. For two of the four cases it was verified in the raw footage that this bin did not in fact represent a fast moving bead passing by but was a fault in the program. Of course for the other two ratios it could be different and indeed be a fast moving bead. The program could be wrong there too, since it will mark any circle with a radius between 1 and 6 pixels. If there is a frame where something is identified as a circle but is not actually a bead, it will be counted in the histogram.

6.2.3 Design 2: asymmetric PFF

Looking at the results an initial separation is best visible at the ratios of 1:7 and 1:9. This, however, does not harmonize with the literature, which suggest ratios in the order of 1:40-60. This discrepancy might arises from the fact that the outlet tubes, all having the same length for both draining channel and outlet channels. These outlet tubes have a length of approximately 30 cm.

The draining channel is designed to have a lower resistance compared to the other outlet channels. However, with the outlet tubes the difference in resistance is, relatively seen, severely decreased. This means that the draining channel hardly works as a draining channel at all. This is supported by the observations made during the experiments. As acknowledge in the results, no mayor flow through the draining outlet tube could be detected and the the chips seem to work best with flow rate ratios similar to the first design. The more asymmetrically the flow is distributed the higher the ratio needs to be for a good sorting. Thus the chip does not seem to have had an very asymmetric flow during the experiments.

As mentioned in the results, beads turning shortly after midway into the first channel could be observed, although they were sorted more for the second channel at first. This might be due to some resistance inconsistency. If one of the other channels next to it had a higher resistance, lots of fluid would pass through the first channel which would cause the observed streamlines. All channels were checked, but no air bubbles or other irregularities, like dust particles, were found. The only problems encountered were pieces of PDMS blocking the pinch segment from time to time, that were consequently flushed out. It was not possible for us to check if any of these PDMS pieces stuck in the outlet tubes afterwards and decreased the resistance, but it is one possible reason for a difference in resistance. The positioning of the outlet tubes might have an effect on the resistance as well, but was not investigated. This is an interesting subject for follow-up research.

The difference between the the streakline images with regard to the overlap of streaklines, as can be seen between the 1:7 and 1:19 ratio, arises probably from the fact that fewer beads passed by while the video was recorded. Furthermore, sometimes several bead clustered came along while making the video. They cause quite large streaklines and therefore quickly create overlap. This was the case for the 1:19 ratio recording.

The fewer streaklines for the higher ratios can be explained by the slow flow ratios. As all recordings are equally long, fewer beads could flow to the pinched segment when lower flow rates were applied for the bead solution. Moreover, the 20 μm beads appear to be rather heavy and like to stick to the surface, both factors favoured by a slow flow rate. Thus the little appearance of 20 μm beads might be explained for the higher flow rate ratios. It was not an issue of mixing the beads because this was done right before the recordings were taken.

The beads seem to go nearly everywhere for the 1:5 ratio. This is probably because they are not neatly aligned at the wall because the buffer solution is not pushing them enough against the wall. This also explains the random paths of both beads.
Another point that attracts attention is the great presence of beads. A reason for this might be that the flow rate of the bead solution is highest with the lowest ratio and a constant total flow rate. Assuming for all recordings the same bead concentration and distribution, one can conclude that for the lowest ratio the most beads were transported towards the pinched segment.

The efficiency analysis could not be made for the second design because of a too low magnification with which the recordings were taken. When running the script it identifies a few 20 μm beads were there are non, but a lot of six that are not present and only few of the actually present 6 μm beads. The obvious solution for this problem would be to record the videos at a higher magnification. However, this had as a consequence that only the first outlet channel could be observed. With other words, the video would have been useless as not all path of the beads would have been recorded. This design is therefore not suitable for the efficiency analysis with the used Matlab script.

To investigate if an actual separation into two different channels is possible with this design, further experiments need to be done in which the resistance of the outlet tubes need to be the same and the outlet tube of the draining channel needs to be shortened. In this way the asymmetric pinched flow fractionation can actually be tested.

6.3 Concentration

The concentration determined with the cell counting chamber method differs especially for the 6 μm beads a lot form the calculated concentration. This could be because the larger beads are heavier and sink very quickly, so less 20 μm beads might have been pipetted onto the cell chamber compared to the 6 μm beads. It also needs to be said that the sample from the syringe taken was the last bit of solution in the syringe. The beads that were stuck in the tubes throughout the experiment was also dumped in. This sample might be higher concentrated than the actual solution because the liquid was forced out during the experiments, but the beads tend to sink to the bottom or stick to the walls of the syringe. Last made regular mixing of the solution in the syringe necessary, but observed phenomenon could not be prevented completely.

For both designs concentrations in the order of several 1000 beads/μL were used. The egg concentration would actually be around the 1.2 eggs/μL or smaller, as mentioned in the introduction. It was already acknowledged in the discussion that there were problems with bead clusters. This problem gets worse with higher concentrations, and can be decreased by using lower concentrations. The technique of PFF itself does not require a minimum of particles (of course no sorting can take place with no particles), therefore a low concentration should not effect the separation and is only in favour of PFF, as it minimizes the chance of cluster forming.

6.4 Detection

The measurements for each concentration were done several times to check if the value of the current was the same. During that time, it was observed that the value of the current was different despite of the fact that the concentration on the channel was the same. That unstable behaviour was due to a phenomenon called thermal noise. During the time that the electric circuit was active, the temperature of the resistors were increasing and thus the current value was decreasing. This problem could be solved by leaving the electric circuit active for few minutes, so that the resistors would converge to a temperature value.

One of the two main problem was the fluctuation of temperature inside the room, which affects the temperature of the electric circuit. As a result, the resistance was fluctuating and consequently the current was fluctuating as well. That can also be seen in all the tables with data. The solution to this problem would be to do the measurements on a room with controlled temperature. The other problem was the alignment of the channel with the top of the cone. That was done manually for every measurement. The alignment on the Y-axes was fixed by using two "stoping points" whereas for the X-axes that had to be done with human eye. That also contributes to the error.

Some focus should be placed also on the height of the channel. From the results of the table 6 where a tube was used, it can be seen that a larger value of height in the channel contributes to a more accurate result. So, higher value of height gives higher value of absorbance. It was also noticed during the experiments that the darker the color in the channels (with the beads being red), the higher the concentration of the beads. The turbidity, or the cloudiness, of the solution is comparable to the concentration of the solution. The more turbid, the higher the concentration, resulting in a higher solution absorbance, which in turns lowers the current.

The set-up described in section 3.3 was used because of the low-cost and accessibility of materials. For the final device, further changes would need to be implemented, as the set-up would need to be put into a smaller contained environment. For all the different concentrations beads of 6 micrometre size where used instead of eggs from the parasites.
During the measurements the lowest concentration that was tried was 365 beads per microliter. As it can be seen in the table 7 for the 365 $\frac{beads}{u \cdot L}$, the photoresistor can detect 2 out of 3 times that the concentration has increased. More investigation should be done on lower concentrations. Comparing the lower concentration that has been measured with the minimum concentration of $0.025 \frac{eggs}{u \cdot L}$ there is a factor of 14600 dilution difference.

6.5 Implementation

Overall, PFF is viable for the implementation to a measurement device for diagnosing parasitic infections in horses, but it is uncertain whether if optical detection is truly viable. The turbidity of the faecal solution includes also more particles than only parasitic eggs which have pass the filtration.

Nevertheless, improvements are needed for successful combination of separation and detection.

For a final device, the design would have to be created in such a way that the optical detection set-up is scaled down and contains fixation for intensifying light (instead of aluminium foil cones). This can be done with integrated circuits and 3D printed designs for fixed alignments. Materials chosen for the design of the final device should also consider insulation and light containment for minimizing thermal and environmental noise for optical detection. With an insulating material, the temperature within the device should fluctuate less, resulting in more precise optical detection measurements. With a light containment material, noise from the light in the environment also has less of an effect on the measurements of optical detection.

For better overall implementation, a reader program would have to be written for calculating and performing analysis of chip measurements. Further research should be done to statistically analyse the accuracy of the chip. This analysis should then be implemented into the calculation and analysis of the reader program, possibly with an adjustment value. This adjustment value should accommodate for the error in separation and detection. These errors could occur from the overlap in size of different parasite eggs, resulting in eggs separated into wrong outlet channels, or from multiple eggs attached to each other.

It has been observed that PFF works best at lower concentrations of beads, but optical concentration works best for higher concentration of beads. Because of this, it is important to test both of the techniques at the same time, which has not yet been done. By doing so, the compatibility of both these methods in one device can then be seen. If they are compatible, different concentrations should be tested to evaluate the overall performance. A calibration graph could possibly be created for different concentrations. Otherwise, research needs to be done to see if optical detection can be optimized to work for low concentrations.

To improve the implementation, further testing of chips should be done with actual horse faeces. Statistical analysis should be drawn from this experiment as well, as some worms may not be in faeces and the amount of errors and bias should be calculated. Testing the chip with actual horse faeces will also produce more realistic and reliable results, as the beads currently used are not completely representative of parasite eggs.

Further research should also be done to see the differences between the bead solution used in this experiment and the actual faecal solutions to be used in the final device.

7 Conclusion

In this sections the conclusions for each part of the chip are presented in the different subsections. At the end a overall conclusion is given.

7.1 Separation

7.1.1 Design 1: PFF

The first design has shown promising results, although the separation into two separate channels was not achieved.

From the percentage of separated particles presented in the results, the ratios of 1:9 and 1:20 are concluded as the best ratios. The large difference between these ratios cannot be explained and is an interesting subject for follow-up research.

7.1.2 Design 2: asymmetric PFF

A separation into the first and second outlet channel was not achieved, but a separation of particles could be seen in the broadening segment. This initial separation appears to be best at a ratio around 1:7 to 1:9. It can be concluded that the actual effect of the asymmetric design was not tested. Thus further research needs to be done to evaluate the asymmetric pinched flow fractionation and its usefulness for the home-test device.

7.2 Detection

By looking at the results, it can be concluded that by using the optical detection method, differences can be indicated between different concentrations. Further investigation is needed in a fixed temperature environment. By keeping the temperature stable the limits of the detection with respect to the height of the channel and the concentration of the solution can be found. It can not yet be concluded whether the technique of optical detection can be used in the design of an endoparasite home-test device, as the testing environment during the experiments was not representative for the actual environment faecal solutions with parasite eggs concentration - the tested concentration was not low enough (discussed in section 6.3 and 6.4).

7.3 Suitability for endoparasite home-test

All in all it can be concluded that the PFF as separation technique seems to be an good option. According to theory the asymmetric PFF is more promising as it can sort beads similar in size better than PFF. The effect of the asymmetry was in our research not tested well. Furthermore, the efficiency analysis was only done for the first design. The results are therefore inconclusive of which of the two designs is best, but the PFF in general seems a promising technique for the separation of the eggs. The optical detection requires a high concentration to work well. The egg concentration is really low, therefore the optical detection might not be the best solution for the detection.

7.4 Recommendations

For the overall combination of PFF separation and optical solution, the viability is currently inconclusive as both methods have not yet been implemented together at once. Further experiments would still need to be done to draw a complete conclusion. Even though multiple experiments can still be done to improve the design foundations for the final device, some points of recommendations can already be introduced and are proposed in this section.

For the final device, a reader program would have to be written to perform the necessary calculations to determine the concentration of eggs. It must be able to translate the outputs from the detection into an understandable result, serving as an interface between the chip and the user. The reader should output a message to the user informing them if their horse is infected with parasites or not and if so, what kind. There could be a result of 'possibly infected', as there is overlap in the sizes of the parasitic eggs. The calculations in this reader program should also include the adjustment values from statistical error analysis as mentioned in the discussion section 6.5.

As discussed, the materials for the design of the device should also be carefully chosen, such that the device can serve as a suitable container for optical detection. This means that the material is slightly insulated and blocks external light, preventing thermal and environmental noises as much as possible.

For the process as a whole, the horse faecal sample should not be directly put into the chip. It is recommended to do a filtration prior to using the chip to filter out any debris smaller or larger than the eggs; thus, reducing the chances of clogging the chip and making the output of the detection more accurate.

It is also recommended for each chip to be used only once. This will prevent the hatching and growth of parasite eggs, promoting health and cleanliness.

Even though there are multiple points of improvements for the device, with the techniques of PFF and optical detection (if deemed compatible together with future research), producing a device that sells at a reasonable price is highly viable. This is an important factor for the overall goal of the project and has influenced multiple decision factors of the designs used in this experiment. Further research can also be done into the possibility of using low-cost research for detection.

References

[1] Enpevet. Endoparasites;Available from: `http://www.enpevet.de/Lexicon/ShowArticle.aspx?articleid=41092&language=en&noop`.

[2] fivet. Endoparasites of Horses;Available from: `http://www.fivetanimalhealth.com/tech/endoparasites-horses`.

[3] Sloss MW, Kemp RL, Zajac AM, et al. Veterinary clinical parasitology. Ed. 6. Iowa State University Press; 1994.

[4] David ED, Lindquist WD. Determination of the specific gravity of certain helminth eggs using sucrose density gradient centrifugation. The Journal of parasitology. 1982;p. 916–919.

[5] Your Worm Count Results Explained. Westgate Laboratories. 2017 cited:30-01;Available from: `http://www.westgatelabs.co.uk/info/wormcount-results-explained`.

[6] Daw R, Finkelstein J. Lab on a chip. Nature. 2006;442(7101):367–367.

[7] Wyatt Shields IV C, Reyes CD, Lopez GP. Microfluidic cell sorting: a review of the advances in the separation of cells from debulking to rare cell isolation. Lab Chip. 2015;15:1230–1249.

[8] Yamada M, Nakashima M, Seki M. Pinched Flow Fractionation: Continuous Size Separation of Particles Utilizing a Laminar Flow Profile in a Pinched Microchannel. Analytical Chemistry. 2004;76(18):5465–5471.

[9] Pamme N. Continuous flow separations in microfluidic devices. Lab Chip. 2007;7:1644–1659.

[10] Guan G, Wu L, Bhagat AA, Li Z, Chen PCY, Chao S, et al. Spiral microchannel with rectangular and trapezoidal cross-sections for size based particle separation. Scientific Reports. 2013;3:1475.

[11] Kuntaegowdanahalli SS, Bhagat AAS, Kumar G, Papautsky I. Inertial microfluidics for continuous particle separation in spiral microchannels. Lab Chip. 2009;9:2973–2980.

[12] Jimenez M, Miller B, Bridle HL. Efficient separation of small microparticles at high flowrates using spiral channels: Application to waterborne pathogens. Chemical Engineering Science. 2017;157:247 – 254.

[13] Brown A, Betts W, Harrison A, O'Neill J. Evaluation of a dielectrophoretic bacterial counting technique. Biosensors and Bioelectronics. 1999;14(3):341–351.

[14] Histogram plot;Available from: `https://nl.mathworks.com/help/matlab/ref/histogram.html#description`.

[15] Takagi J, Yamada M, Yasuda M, Seki M. Continuous particle separation in a microchannel having asymmetrically arranged multiple branches. Lab Chip. 2005;5:778–784.

[16] Counting chambers. Brand;. Available from: `http://www.brand.de/fileadmin/user/pdf/GK900/Zaehlkammern/GK900_05_Clinical_Lab_Zaehlkammern_e.pdf`.

A   Appendix

A.1   Additional figures
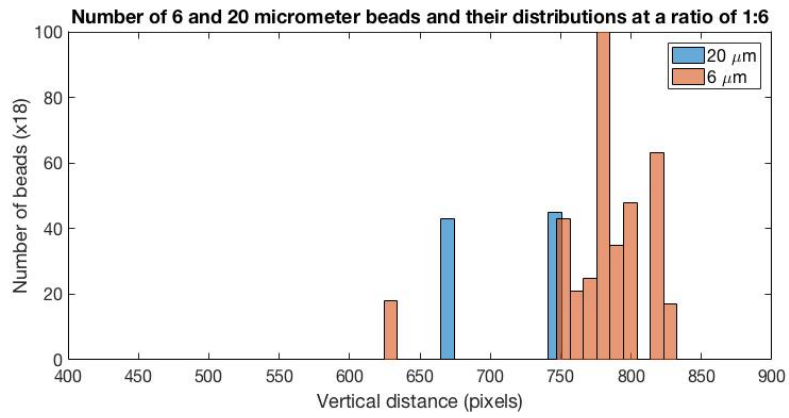

Figure 31: Histogram of the ratio 1:6. PSP6 = 77.4%, PSP20 = 0%

In this section you will find the additional figures that were not featured in the results. These include the figures for the ratios of 1:6 (figure 31), 1:10 (figure 32) and 1:14 (figure 33).
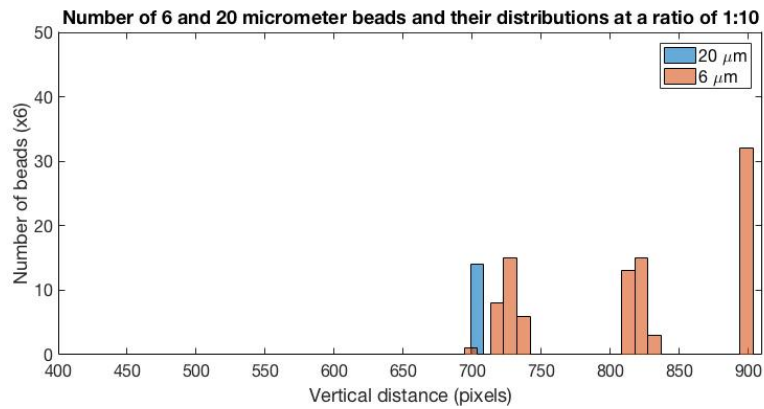

Figure 32: Histogram of the ratio 1:10. PSP6 = 100%, PSP20 = 100%
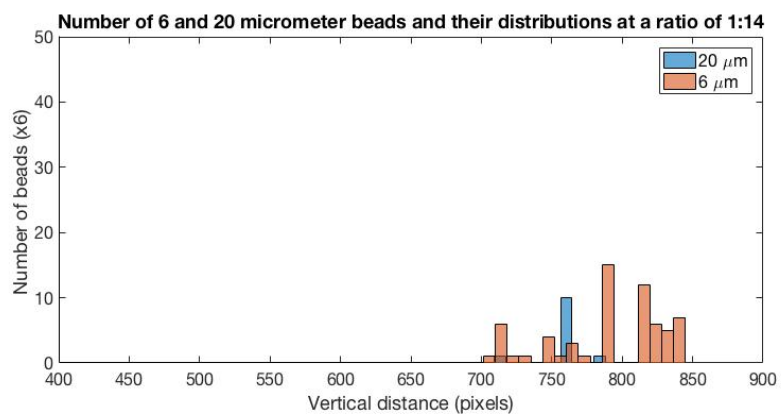
Figure 33: Histogram of the ratio 1:14. PSP6 = 71.4%, PSP20 = 0%

A.2 MATLAB scripts

A.2.1 Intensity plots

```matlab
1    clear; close all; clc;
2
3  filedir = uigetdir;                    % this line gives a screen to open
       a directory
4  list = dir(filedir);                   % this makes a list of the
       directory that you can access in the for loop
5  filenumber = length(list)-2;           % number of files in the list (
       excluding the . and .. files)
6  ending = filenumber-1;                 % to automitize the for loop, needs
        to be -1 because image B is i+1 and if it takes the last image,
       the image(i+1) doesn't exist
7
8  Dold = 0;                              % for the first addition in the for
        loop, because there is no difference image then yet
9  Th = 15;                              % threshold found by taking the
       mesh of the non-normalized first difference image (set i=3:4 and
       take mesh of E)
10
11
12  for i=4:ending;                       % the for loop runs
       from 3 until the ending
13      A=imread([filedir,'/',list(i).name]);       % A is the first
           image you call using the directory
14      B=imread([filedir,'/',list(i+1).name]);     % B the second
15      C = imabsdiff(A,B);                          % take the
           difference between A and B
16      C = double(C);                              % make a double
           otherwise numbers above 256 will be made into 256, which means
           you lose information
17      D = (Dold+C);                               % add the old
           difference image to the new one (the addition will connect the
           beads into a line)
18      for j=1:length(D);                           % make a for loop to
            get rid of the background noise in each individual image in
           the for loop
19          for k=1:length(D);                       % you need a 1024
               x1024 double, so you have to take two for loops, otherwise
               you get 1x1024
20              if D(j,k)>Th;                        % if the intensity
                   value of the image D on the point j,k is higher than
                   the threshold, the pixel in the new image created (E)
                   keeps that value
21                  E(j,k)=D(j,k);
22              else
23                  E(j,k)=0;                        % if the value is
                       lower than the threshold, the pixel is made black
                       in E
24
25              end
26          end
27      end
28      Dold=E;                                      % make the image the
           old image so that it can be added to the next
29  end
30
```

41

```
31  U = E/(max(max(E)));                        % normalize the final image
        by dividing it by the maximum value (the max will be 1 and the rest
         will be a number in between 0 and 1)
32  figure(1)                                   % if you don't normalize, you
        will have numbers above 256, which cannot be shown in the image as
        anything other than the brightest white (256)
33  imshow(U)
34
35  P = imread([filedir,'/',list(6).name]);    % read in the image to add
        the background to U
36  P = double(P)/256;                          % divide by 256 because you
        need all of the numbers to be between 0 and 1 like U
37  Q = imfuse(P,U);                            % overlay the U image with P
        to get the outline of the chip in there
38  I = rgb2gray(Q);                            % imfuse has a default
        coloring, with this you make the image grayscale again
39  figure(2)
40  imshow(I)
```

A.2.2   Particle identification

```
1       clear; close all; clc; hold on
2
3  % Make a directory and load the files into a list
4
5  filedir = uigetdir;
6  list = dir(filedir);
7  filenumber = length(list)-2;
8  ending = filenumber-1;
9  warning('off','all');              % the function imfindcircles gives a
        warning when the radius is smaller or equal to 5, which is annoying
         so this turns it off
10
11 % Define necessary parameters
12 nubins = 100;
13
14 % For-loop to call the images and find the centers of the beads
15
16 for i = 4:ending;
17     B = imread([filedir,'/',list(i).name]);
18     A = B(:,300:350);
19     [center20 radii] = imfindcircles(A,[7 20],'objectpolarity','dark');
20     [center6 radii6] = imfindcircles(A,[1 6],'objectpolarity','dark');
21     coordinatesperframe20{i-3,1} = center20;            % this stores
            the coordinates that imfindcircles found into a cell array. It'
            s i-3 since the for-loop starts at 4, which leads to 3 empty
            cells
22     coordinatesperframe6{i-3,1} = center6;
23 end
24
25 % For-loops to take the x- and y-coordinates out of coordinatesperframe
        and
26 % store them in a double to be used for plotting
27
28 for l = 1:length(coordinatesperframe20);
29     for m = 1:size(coordinatesperframe20{l,1},1);
30
```

```matlab
31            x20(m,l) = coordinatesperframe20{l,1}(m,1);
32            y20(m,l) = coordinatesperframe20{l,1}(m,2);
33        end
34    end
35
36    for  ll = 1:length(coordinatesperframe6);
37        for mm = 1:size(coordinatesperframe6{ll,1},1);
38
39            x6(mm,ll) = coordinatesperframe6{ll,1}(mm,1);
40            y6(mm,ll) = coordinatesperframe6{ll,1}(mm,2);
41        end
42    end
43
44    % Show the slice of the image so that the found beads can be plotted on
            top
45    % of that, using the hold on command
46
47    imshow(A)
48    hold on
49
50    for p = 1:length(x20);
51        plot(x20(1:size(x20,1),p),y20(1:size(x20,1),p),'o','color','b')
52
53    end
54
55    for p = 1:length(x6);
56        plot(x6(1:size(x6,1),p),y6(1:size(x6,1),p),'*','color','r')
57
58    end
59
60    % Make the histograms of the two beads, the axis are variable for each
61    % movie so the limits need to be changed every time
62
63    figure(2)
64    h20 = histogram(y20,nubins);
65    axis([350 900 0 50])
66    hold on
67    h6 = histogram(y6,nubins);
68    axis([350 900 0 50])
69    title('Number of 6 and 20 micrometer beads and their distributions')
70    legend('20 \mum','6 \mum')
```